Tectonics

RESEARCH ARTICLE
10.1029/2018TC005010

Key Points:
- We present new paleomagnetic data from Eocene-Miocene sedimentary rocks in Kutai Basin, Borneo, and compile all available paleomagnetic data from Mesozoic and Cenozoic rocks in Sundaland and Borneo
- We compare reconstructed trenches with seismic tomography to evaluate the regional or local nature of paleomagnetic results
- We provide a kinematic restoration of Borneo and Sundaland since the Eocene that is consistent with paleomagnetism and tomography

Supporting Information:
- Supporting Information S1
- Table S1
- Data Set S1
- Data Set S2
- Data Set S3
- Data Set S4
- Data Set S5
- Data Set S6

Correspondence to:
E. L. Advokaat,
e.l.advokaat@uu.nl

Citation:
Advokaat, E. L., Marshall, N. T., Li, S., Spakman, W., Krijgsman, W., & van Hinsbergen, D. J. J. (2018). Cenozoic rotation history of Borneo and Sundaland, SE Asia revealed by paleomagnetism, seismic tomography, and kinematic reconstruction. *Tectonics*, *37*, 2486–2512. https://doi.org/10.1029/2018TC005010

Received 31 JAN 2018
Accepted 29 JUN 2018
Accepted article online 6 JUL 2018
Published online 12 AUG 2018

Cenozoic Rotation History of Borneo and Sundaland, SE Asia Revealed by Paleomagnetism, Seismic Tomography, and Kinematic Reconstruction

Eldert L. Advokaat[1], Nathan T. Marshall[1], Shihu Li[2], Wim Spakman[1,3], Wout Krijgsman[1], and Douwe J. J. van Hinsbergen[1]

[1]Department of Earth Sciences, Utrecht University, Utrecht, Netherlands, [2]State Key Laboratory of Lithospheric Evolution, Institute of Geology and Geophysics, Chinese Academy of Sciences, Beijing, China, [3]Centre of Earth Evolution and Dynamics, University of Oslo, Oslo, Norway

Abstract SE Asia comprises a heterogeneous assemblage of fragments derived from Cathaysia (Eurasia) in the north and Gondwana in the south, separated by suture zones representing closed former ocean basins. The western part of the region comprises Sundaland, which was formed by Late Permian-Triassic amalgamation of continental and arc fragments now found in Indochina, the Thai Penisula, Peninsular Malaysia, and Sumatra. On Borneo, the Kuching Zone formed the eastern margin of Sundaland since the Triassic. To the SE of the Kuching Zone, the Gondwana-derived continental fragments of SW Borneo and East Kalimantan accreted in the Cretaceous. South China-derived fragments accreted to north of the Kuching Zone in the Miocene. Deciphering this complex geodynamic history of SE Asia requires restoration of its deformation history, but quantitative constraints are often sparse. Paleomagnetism may provide such constraints. Previous paleomagnetic studies demonstrated that Sundaland and fragments in Borneo underwent vertical axis rotations since the Cretaceous. We provide new paleomagnetic data from Eocene-Miocene sedimentary rocks in the Kutai Basin, east Borneo, and critically reevaluate the published database, omitting sites that do not pass widely used, up-to-date reliability criteria. We use the resulting database to develop an updated kinematic restoration. We test the regional or local nature of paleomagnetic rotations against fits between the restored orientation of the Sunda Trench and seismic tomography images of the associated slabs. Paleomagnetic data and mantle tomography of the Sunda slab indicate that Sundaland did not experience significant vertical axis rotations since the Late Jurassic. Paleomagnetic data show that Borneo underwent a ~35° counterclockwise rotation constrained to the Late Eocene and an additional ~10° counterclockwise rotation since the Early Miocene. How this rotation was accommodated relative to Sundaland is enigmatic but likely involved distributed extension in the West Java Sea between Borneo and Sumatra. This Late Eocene-Early Oligocene rotation is contemporaneous with and may have been driven by a marked change in motion of Australia relative to Eurasia, from eastward to northward, which also has led to the initiation of subduction along the eastern Sunda trench and the proto-South China Sea to the south and north of Borneo, respectively.

1. Introduction

SE Asia is located at the juncture where the major plates of Eurasia, India, Australia, and the Pacific interact (Hall, 2002, 2012; Hall & Spakman, 2015; Hamilton, 1979). The region comprises a heterogeneous assemblage of fragments derived from Cathaysia (China) and Gondwana, accreted intraoceanic arcs, and intervening suture zones. The western part of the region comprises the composite Sundaland terrane, which was formed by Late Permian-Triassic amalgamation of continental and arc fragments now found in Indochina, the Thai Peninsula, Peninsular Malaysia, and Sumatra (Figure 1; Metcalfe, 2013). More fragments of oceanic and arc origin, as well as continental fragments now found on Borneo, Java, and Sulawesi (Figure 1), accreted to Sundaland during the Cretaceous and Early Miocene (Hall, 2012; Hall, Clements, & Smyth, 2009; Metcalfe, 2013). Deciphering SE Asia's complex geodynamic history requires detailed quantitative kinematic restoration of deformation (Hall, 2002; Replumaz & Tapponnier, 2003). As Sundaland forms the core to which terranes accreted throughout the Mesozoic and Cenozoic, its movement is vital to understand SE Asian tectonics. Reconstruction of Sundaland's position relative to Indochina and Eurasia provides fundamental constraints to restoration of regions adjacent to Sundaland and Borneo, which include the Andaman Sea, the southwestern margin of Sumatra, the South China Sea, and the eastern Indonesian region (Figure 1).

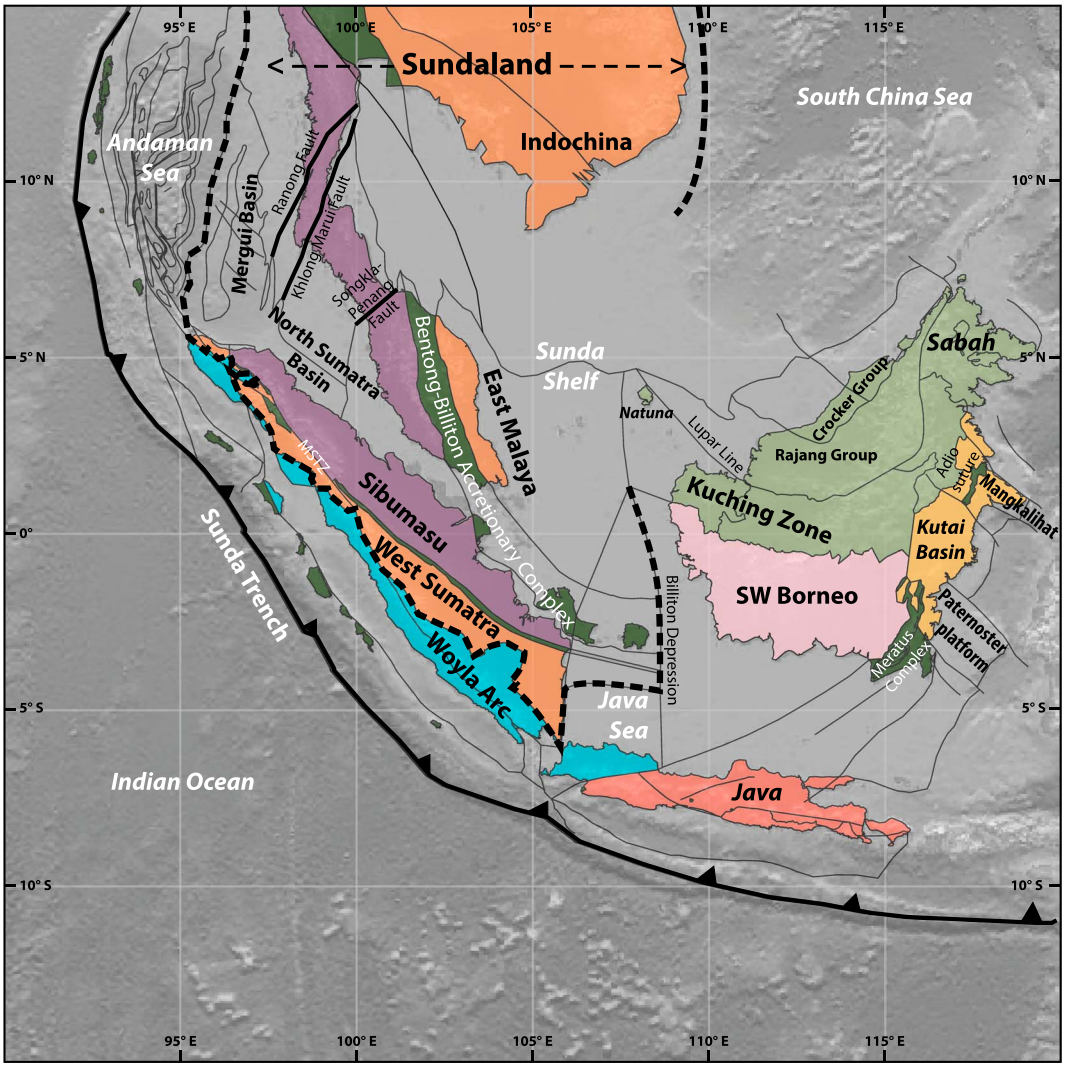

Figure 1. Tectonic map of SE Asia. Sutures and accretionary complexes are indicated in dark green.

Global as well as regional plate reconstructions are best constrained by restoration of ocean basins based on marine magnetic anomalies and transform faults/fracture zones. In deformed continental regions, such constraints are absent and reconstructions are then best made based on quantitative estimates of continental extension, strike-slip displacement, and shortening, in combination with geometric consistency (e.g., Boschman et al., 2014; Van Hinsbergen et al., 2011). Such constraints are sparse in SE Asia. This may be reflected by strongly divergent reconstructions of Cenozoic vertical axis rotations of Sundaland including clockwise (CW) rotations of 10–35° (Lee & Lawver, 1995; Replumaz & Tapponnier, 2003; Royden et al., 2008), counterclockwise (CCW) rotations of 5–30° (Hall, 2002; Richter et al., 1999), or both (Metcalfe, 2013; Otofuji et al., 2017). Much of this variation depends on the interpretation whether Sundaland was rigidly attached to Indochina or whether it rotated relative to Indochina. Reconstructions of rotations in Borneo relative to Eurasia are equally divergent. Lee and Lawver (1995) reconstructed no rotation after 60 Ma, whereas Hall (2002) reconstructed a ~45° CCW rotation between 25 and 10 Ma, based on paleomagnetic data compiled by Fuller et al. (1999). Replumaz and Tapponnier (2003) considered Borneo as rigidly attached to the Malay Pensinsula and reconstructed a ~35° CW rotation at 30–15 Ma related to extrusion of Indochina from the India-Asia collision zone. Royden et al. (2008) even reconstructed a ~45° CCW extension-related rotation of Borneo at 50–20 Ma during extrusion of Indochina.

Paleomagnetic data may constrain the amount and timing of rotation of Borneo and Sundaland, with the caveat of potential remagnetization, as shown for Peninsular Malaysia (Otofuji et al., 2017; Richter et al.,

1999). Paleomagnetic data show that post-Jurassic ~90° CCW rotation affected at least some of the terranes of Borneo (Fuller et al., 1999; Schmidtke et al., 1990; Sunata & Wahyono, 1987; Wahyono & Sunata, 1987). The available paleomagnetic data for the Cenozoic are mainly obtained from igneous rocks that lack bedding control (Fuller et al., 1999; Schmidtke et al., 1990), but the timing and magnitude of rotation remain controversial, due to the poor age control and ambiguous interpretation of paleomagnetic results.

Here we aim to constrain the pattern, magnitude, and timing of Cenozoic rotations in Sundaland and Borneo and use these to improve kinematic restorations of SE Asia based on structural geological constraints. Since Eocene and younger rotations are particularly key to evaluate the validity of the reconstructions mentioned above, we here utilize paleomagnetic directions obtained from a detailed magnetostratigraphic sampling study (Marshall et al., 2015) and new paleomagnetic data from Upper Eocene-Upper Miocene sediments in the Kutai Basin, eastern Borneo (Figure 1). In addition, we compile all available previously published paleomagnetic data from Sundaland and Borneo using updated age constraints based on more recent literature. We use these paleomagnetic data to kinematically restore Cenozoic tectonic motions of the core of SE Asia relative to Indochina. Because Sundaland is a large elongated block, any rotation of this block has a direct effect on the orientation of the Sunda trench that bounds the block in the southwest. We test regional validity of paleomagnetic data for kinematic restorations by comparing the position of the Sunda trench in the restoration with seismic tomographic images of the Sunda slab (Fukao & Obayashi, 2013; Hall & Spakman, 2015; Koulakov, 2013; Pesicek et al., 2010; Replumaz et al., 2004; van der Meer et al., 2017; Widiyantoro et al., 2011; Widiyantoro & van der Hilst, 1996, 1997). We then evaluate the kinematic implication of reconstruction and discuss possible driving mechanisms for rotations in Borneo.

2. Geologic Setting

Below, we provide a review of the geology of Sundaland and Borneo, which provides the structural constraints for our restoration. The continental and arc fragments and intervening fault zones and sutures of Sundaland and Borneo are unconformably covered by sedimentary basins. We review the age and nature of the different fragments and basins and evaluate the age of suturing, focusing on age constraints on the matrix of mélange complexes in these suture zones. Furthermore, we review constraints on the amount and timing of displacement of major fault zones.

2.1. Sundaland

Sundaland comprises the Gondwana-derived continental fragments of East Malaya, Sibumasu, and West Sumatra, which are respectively separated by the intervening Bentong-Billiton Accretionary Complex and the Medial Sumatran Tectonic Zone (Figure 1). These fragments were amalgamated to form Sundaland in the Permian and Triassic (Barber et al., 2005; Barber & Crow, 2009; Metcalfe, 2013). Widespread Late Triassic magmatism is interpreted to be associated with collision between Sibumasu and East Malaya (Metcalfe, 2013). Upper Jurassic-Lower Cretaceous continental redbeds unconformably cover older sequences in Peninsular Malaysia (Abdullah, 2009).

Thermochronology from the Malay Peninsula indicated thermotectonic events in the Late Cretaceous-Paleocene and the Eocene-Oligocene (Cottam et al., 2013; François et al., 2017; Krähenbuhl, 1991), coinciding with a widespread regional unconformity that may relate to cessation and subsequent reinitiation of subduction below Sundaland (Clements et al., 2011). Deformation within Sundaland during this time interval includes folding in the Late Cretaceous-Paleocene (Harbury et al., 1990; Tjia, 1996), extensional exhumation of metamorphic complexes during the Late Cretaceous, and renewed exhumation during dextral NNW-SSE to WNW-ESE strike-slip faulting and later transpression in the Late Eocene-Early Oligocene (Ali et al., 2016; François et al., 2017; Harun, 2002).

Sundaland is attached to Indochina and is crosscut by the Ranong, Khlong Marui, and Songkla-Penang Faults (Figure 1). Early studies of the Ranong fault estimated 20-km sinistral displacement between 111 and 65 Ma (Garson & Mitchell, 1970) to at least 200-km dextral displacement in the middle Cenozoic (Tapponnier et al., 1986). Similarly, for the Khlong Marui Fault there are estimates of 200-km sinistral displacement between 111 and 65 Ma, based on offsets of the Tin Belt granites (Garson & Mitchell, 1970), and 100-km dextral displacement in the Eocene-Oligocene (Morley, 2002). More recent studies (Kanjanapayont, Grasemann, et al., 2012; Kanjanapayont, Klötzli, et al., 2012; Ridd & Watkinson, 2013; Watkinson, 2009; Watkinson et al.,

2008, 2011) identified a long history of shear activity. Watkinson (2009) reconstructed displacements via boudin restoration following the method of Lacassin et al. (1993). Based on constraints from structural observations (Kanjanapayont, Grasemann, et al., 2012; Watkinson et al., 2008), kinematic restorations (Watkinson, 2009) and radiometric ages (Kanjanapayont, Klötzli, et al., 2012; Watkinson et al., 2011), the shearing history of the Ranong and Khlong Marui Faults includes a first phase with dextral displacements of 23 km on the Ranong Fault and 6 km on the Khlong Marui Fault between 88 and 81 Ma. More dextral shearing occurred between 59 and 40 Ma, with displacements of 113 and 31 km on the Ranong and Khlong Marui Faults, respectively. Two mylonite samples close to brittle fault strands of the Khlong Marui Fault yielded $^{40}Ar/^{39}Ar$ biotite ages of 37.5 ± 0.3 and 37.1 ± 0.3 Ma (Watkinson et al., 2011), which provide the lower bound on this phase of dextral shear activity. Alternatively, they date the onset of brittle sinistral transpression where these ages are interpreted to be reset by fluid circulation along the brittle fault strands. These sinistral displacements are 66 and 20 km for the Ranong and Khlong Marui Faults (Watkinson, 2009). Mica whole rocks Rb/Sr isochrons of 38.3–22.6 Ma from the Khlong Marui Fault (Kanjanapayont, Klötzli, et al., 2012) likely also date this event (I.M. Watkinson, personal communication, 27 February 2017). The Songkla-Penang Fault (Bunopas, 1982) south of the Ranong and Khlong Marui faults is inferred to have accommodated differential rotations between the Thai Peninsula and Peninsular Malaysia in the Cenozoic (Richter et al., 1999).

In the east, Sundaland is truncated by the Billiton Depression, a N-S trending transform fault running south of Natuna (Ben-Avraham & Emery, 1973; Ben-Avraham & Uyeda, 1973; Figure 1). Hall, Clements, and Smyth (2009) and Hall (2012) proposed that the Billiton Depression is a suture separating SW Borneo from Sundaland, but recent studies suggest that the suture between Sundaland and Borneo may be located onshore west Borneo (Breitfeld et al., 2017). N-S trending normal faults of Late Eocene-Early Oligocene age in the western Java Sea are associated with the Billiton depression and indicate a component of E-W extension (Barber & Crow, 2005; Cole & Crittenden, 1997).

2.2. Borneo

Borneo is characterized by multiple continental and arc fragments separated by Mesozoic-Cenozoic ophiolites, mélange complexes, sutures, and fault zones, which are unconformably overlain by Cenozoic basins (Breitfeld et al., 2017; Haile, 1973; Hutchison, 1986; Metcalfe, 1990; Figure 1). Fragments include the Kuching Zone (Haile, 1973; Metcalfe, 1990, 2013) and Gondwana-derived fragments in SW Borneo and eastern Borneo that accreted to Sundaland in the Late Cretaceous (Hall, 2012). Below we provide a review focusing on age constraints of geologic units and the age of suturing between the different fragments.

2.2.1. Kuching Zone

The Kuching Zone (Haile, 1973) has an ESE-WNW trending structural grain (Figure 1b). It comprises an amalgamation of Paleozoic-Mesozoic basement rocks and sediments and the Upper Cretaceous Boyan Mélange Complex (Breitfeld et al., 2017; Metcalfe, 1990; Williams et al., 1986). Upper Cretaceous-Upper Eocene basins and younger basins unconformably cover the Paleozoic-Mesozoic rocks of the Kuching Zone (Williams et al., 1986, 1988). Locally, these are intruded by small-scale Oligocene-Miocene stocks (Fuller et al., 1999; Williams & Harahap, 1987).

The northern demarcation is formed by the Lupar Line (Haile, 1973). The Lupar Line includes the Lubok Antu Mélange in the west and the Kapuas Mélange in the east. The Lubok Antu Mélange (Tan, 1982) is in fault contact with the Ketungau Basin and comprises blocks of sedimentary, basic igneous rocks, chert, and limestone in a sheared scaly matrix. Chert block in the mélange yielded Valinginian-Barremian (Lower Cretaceous) and Albian-Cenomanian (mid-Cretaceous) ages. Blocks of sandstone yielded Campanian-Maastrichtian (Upper Cretaceous) ages (Haile, 1996; Jasin & Haile, 1993; Tan, 1979). Nannofossils in the matrix of the Lubok Antu Mélange yielded a Cenozoic, younger than Paleocene, age (Tan, 1979). The Lubok Antu Mélange is overlain by the Middle Eocene Silantek Formation (Haile, 1996).

The Kuching Zone is interpreted as a Mesozoic accretionary complex, which includes units derived from Cathaysia (Eurasia; Breitfeld et al., 2017; Metcalfe, 1990). It is thought to have recorded Late Cretaceous southward subduction (Williams et al., 1988).

2.2.2. SW Borneo

SW Borneo comprises a Mesozoic basement of metamorphic and magmatic rocks exposed in the Schwaner Mountains (Davies et al., 2014; Haile et al., 1977; Hennig et al., 2017; Setiawan et al., 2013; Figure 1b). Sensitive

high-resolution ion microprobe (SHRIMP) U-Pb zircon dating of metamorphic rocks yielded Cretaceous (130–85 Ma) ages and inherited detrital cores of Jurassic to Proterozoic age (Davies et al., 2014).

The Barito Basin is located to the south of the Schwaner Mountains. The Eocene (Bartonian)-Lower Oligocene (Rupelian) terrestrial Tanjung Formation represents the base of the Barito Basin and is overlain by the transgressive fluviodeltaic to shallow marine sediments of Late Oligocene to present age (Witts et al., 2011, 2012).

SW Borneo is interpreted as a Gondwana-derived continental fragment that rifted from Australia in the Mesozoic, recorded magmatism and metamorphism related to southward subduction along its northern margin in the Cretaceous, and accreted to Sundaland in the Cretaceous (Davies et al., 2014; Hall, 2012; Hall, Clements, & Smyth, 2009).

2.2.3. Meratus Complex

The Meratus Complex (Figure 1) exposes high-pressure metamorphic rocks, ultramafic rocks generally ascribed as ophiolite relics, and black shale-matrix mélanges with fragments of Jurassic-Cretaceous chert, limestone, and basalt. These are unconformably overlain by Cretaceous (Aptian-Cenomanian) volcanics and volcaniclastic formations (Heryanto et al., 1994; Monnier et al., 1999; Parkinson et al., 1998; Priyomarsono, 1985; Sikumbang, 1986; Sikumbang & Heryanto, 1994; Wakita et al., 1998; Yuwono et al., 1988).

The Meratus Complex is interpreted as a Cretaceous subduction complex, which forms the suture between SW Borneo and the Paternoster microcontinental fragment (see section 2.2.4; Hall, 2012; Hall, Clements, & Smyth, 2009; Parkinson et al., 1998; Wakita et al., 1998). It is unconformably covered by the Upper Eocene (Bartonian)-Lower Oligocene (Rupelian) Tanjung Formation (Witts et al., 2011, 2012).

2.2.4. Eastern Borneo

Eastern Borneo comprises the Mangkalihat and Paternoster microcontinental fragments (Hutchison, 1989; Metcalfe, 1990; Figure 1). In the south, the Meratus Complex forms the suture between the Paternoster fragment and SW Borneo. In the north, mélanges separate Mangkalihat from the Kuching Zone (Lefevre et al., 1982). These fragments and sutures are unconformably overlain by sediments of the Kutai Basin.

Float and exposures along the Telen river, a tributary of the Makaham river in the upper Kutai Basin, comprise schists, tin-bearing granites, and early Devonian coral- and stromatoporoid-bearing limestone blocks in Permian debris flows (Lefevre et al., 1982; Rutten, 1940; Sugiaman & Andria, 1999). A single K-Ar age of about 190 Ma from a micaceous quartzite was reported (Hamilton, 1979). Metcalfe (1990) suggested that an island arc existed west of Mangkalihat based in the presence of andesite, dacite, radiolarian chert and limestone (Hutchison, 1989).

The Kutai Basin (Figure 1) unconformably covers the Paleozoic-Mesozoic basement rocks of the Mangkalihat and Paternoster blocks, the Meratus Complex, and the eastern part of the Kuching Zone. The Kutai Basin is interpreted to have formed during middle–late Eocene opening of the Makassar Strait, rifting SW Sulawesi off East Kalimantan (Hall, Cloke, et al., 2009). This is reflected in the lithological transition from coarse conglomerates to a sand and shale in the basal Kuaro Formation, which is of late middle Eocene age (Moss et al., 1997; van de Weerd & Armin, 1992). During the Miocene, a profound increase in sediment supply occurred, thought to relate to crustal thickening, uplift, and volcanism within the Central Kalimantan Mountains (Hall & Nichols, 2002). Today, the bedrock of the Kutai Basin has been folded and faulted because of (ongoing) basin inversion since 14 Ma (Hall & Nichols, 2002; McClay et al., 2000). Seismic studies have demonstrated that the NNE-SSW trending ridges of central eastern Borneo are manifestations of tight linear anticlines and broad open synclines formed by reactivation of rifting-related faults (Chambers & Daley, 1997; Cloke et al., 1999).

2.2.5. Sabah

Sabah exposes the ophiolitic rocks and an Upper Cretaceous-Cenozoic accretionary complex and intervening mélanges (Figure 1). The ophiolite comprises amphibolite, ultramafics, gabbro, basaltic dykes, plagiogranites, basaltic rocks, and radiolarian chert (Asis & Jasin, 2012; Jasin, 1992; Morgan, 1974). Near Telupid, spilite yielded a K-Ar age of 137.54 ± 6.88 Ma (Rangin et al., 1990), while the radiolarian chert yielded an Early Cretaceous (late Valinginian-Barremian) age range (Jasin, 1992; Leong, 1977). Radiolarian chert from other exposures yielded age ranges spanning the Valanginian-Turonian (Asis & Jasin, 2012, and references therein).

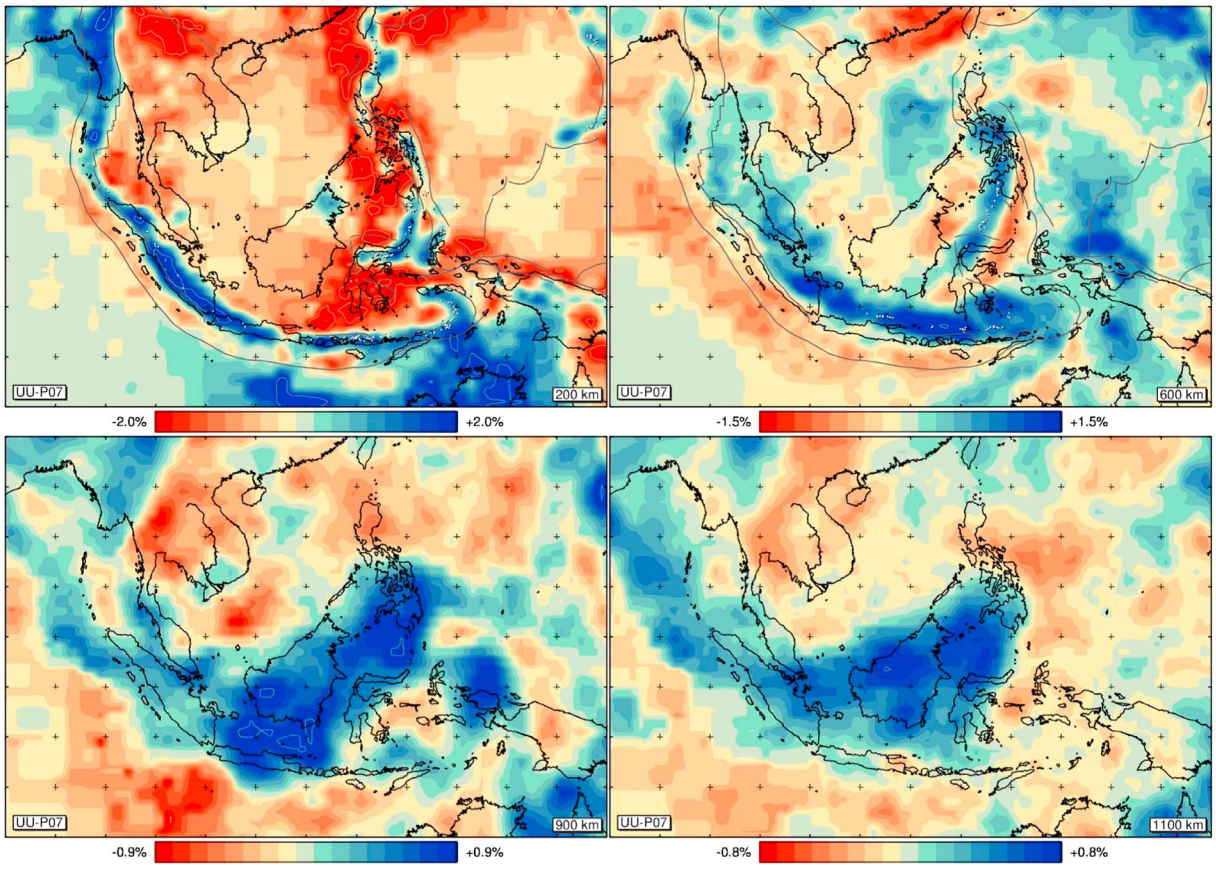

Figure 2. Tomographic slices through the mantle below Sundaland at 200-, 600-, 900-, and 1,100-km depth of the UU-P07 model (Amaru, 2007; Hall & Spakman, 2015; van der Meer et al., 2017, available at www.atlas-of-the-underworld.org).

The Upper Cretaceous to Upper Eocene Rajang Group and the Upper Eocene-Lower Miocene Crocker Group comprise deep water sediments (Hall et al., 2008; Van Hattum et al., 2013; Figure 1b). The Lower Miocene Top-Crocker Unconformity separates the Rajang and Crocker Groups from the overlying Lower Miocene shallow marine sediments of the Kudat Formation (Tongkul, 1994, 2006) and present-day fluviodeltaic sediments. The Top-Crocker Unconformity is interpreted to represent the collision of South China-derived microcontinental fragments with Borneo following the subduction of the proto South China Sea (Hall et al., 2008; Van Hattum et al., 2013).

3. Tomographic Constraints on the Location of the Sunda Slab

Extensive seismic tomography analysis of the upper mantle below Sundaland has demonstrated the existence of an elongated NW-SE trending region of high velocity interpreted as remnants of subducted lithosphere of the Sunda slab (Figure 2). The slab is imaged from the Sunda trench at the surface to upper part of the lower mantle, corresponding to the slab deceleration zone, where positive anomalies are visible until ~1,500 km depth (Fukao et al., 1992; Fukao & Obayashi, 2013; Hall & Spakman, 2015; Koulakov, 2013; Pesicek et al., 2010; Replumaz et al., 2004; van der Meer et al., 2017; Widiyantoro et al., 2011; Widiyantoro & van der Hilst, 1996, 1997). Subduction of the Sunda slab from southern Sumatra eastward is interpreted to have started around 45 Ma based on plate kinematic constraints (Hall, 2012; Hall & Spakman, 2015; Replumaz et al., 2004). Subduction of the Sunda slab below NW Sumatra and farther north may have already started as early as ~90 Ma following subduction polarity reversal after collision of the Woyla intraoceanic arc with Sundaland (Advokaat et al., 2018). Figure 2 shows a series of horizontal slices of the Sunda slab imaged in the UU-P07 tomographic model (Amaru, 2007; Hall & Spakman, 2015; van der Meer et al., 2017, available at www.atlas-of-the-underworld.org), at depths down to 1,100 km.

Table 1
Statistical Parameters of Paleomagnetic Sites From the Kutai Basin, Eastern Borneo

				Bedding					Tilt-corrected parameters								
Site	Latitude	Longitude	Age	Strike/dip	N	N_{45}	D	ΔD_x	I	ΔI_x	K	$A95$	$A95_{min}$	$A95_{max}$	λ	λ_{min}	λ_{max}
Kuaro River	−1.848	116.053	Bartonian-Priabonian	018/24	17	16	351.2	6.5	−8.8	12.7	33.4	6.5	4.0	14.3	−4.4	−11.2	1.9
Berau Coal Mine	2.038	117.451	Burdigalian	260/45	4	4	356.7	24.5	−43.6	28.3	18.4	22.0	6.9	34.2	−25.5	−56.9	−7.8
Samarinda	−0.500	117.140	Langhian-Serravalian														
Batu Putih			16.3–14.5 Ma	024/61	25	21	348.2	6.6	−4.0	13.2	24.0	6.6	3.6	12.0	−2.0	−8.8	4.6
Sungai Kunjang			15–13.5 Ma	026/55	19	19	22.4	5.1	13.2	9.7	45.5	5.0	3.7	12.8	6.7	1.8	11.9
Harapan Baru			13.5–12 Ma	032/55	12	12	13.5	10.8	−0.5	21.6	17.2	10.8	4.4	17.1	−0.2	−11.4	10.9
Stadion			12–11 Ma	040/54	13	13	338.8	8.5	−3.1	17.0	24.7	8.5	4.3	16.3	−1.6	−10.4	7.0
Bontang	0.161	117.434	Tortonian	080/20	9	9	0.5	12.5	3.9	24.9	17.9	12.5	5.0	20.5	2.0	−10.9	15.4

Note. N = total number of interpreted ChRM directions; N_{45} = number of ChRM directions after after 45° cutoff; $D \pm \Delta D_x$ = declination and 95% confidence interval following Butler (1992); $I \pm \Delta I_x$ = inclination and 95% confidence interval following Butler (1992); K = precision parameter of VGP distribution following Fisher (1953); $A95$ = 95% cone of confidence on VGP distribution; $A95_{min}$ and $A95_{max}$ = N-dependent confidence envelope for $A95$ values following Deenen et al. (2011); ChRM = characteristic remanent magnetization; VGP = virtual geomagnetic pole.

These images show that the Sunda slab below Sumatra has a NW-SE orientation throughout its depth range, suggesting that the modern trench orientation has remained more or less stable throughout its subduction history. Toward the east, the deeper sections of the slab anomaly show a change in orientation from E-W to NE-SW, although these deeper portions may relate to different subduction systems, for example, along northern Borneo (van der Meer et al., 2017; Wu & Suppe, 2017). We use the orientation of the Sunda slab to a depth of 1,100 km as shown in Figure 2 as independent test for the orientation of the Sunda trench in our kinematic reconstruction.

4. Paleomagnetism

4.1. Sampling and Laboratory Treatment

In this study, we sampled seven sedimentary successions in four areas in the Kutai Basin, East Kalimantan (Table 1). In the Samarinda area, a 4-km-thick composite succession, composed of four different subsections, was previously sampled for magnetostratigraphic purposes (Marshall et al., 2015). There, samples were taken throughout the succession at intervals ranging from 1 to 10 m or more, depending on the exposure and the presence of suitable lithology. Three additional sections (Kuaro River, Berau Coal Mine, and Bontang) were sampled in the Kutai Basin and are biostratigraphically dated by large benthic foraminifera (LBF; Renema et al., 2015). Paleomagnetic samples were preferably drilled in undeformed shales or mudstones. All samples were collected with an electrical drill powered by a gasoline generator and oriented in situ with a magnetic compass corrected for local declination.

Magnetic remanence of samples was investigated through thermal (TH) and alternating field (AF) demagnetization. AF demagnetization was carried out using an in-house developed robotic 2G Enterprises SQUID magnetometer (noise level 10^{-12} Am^2), through variable field increments (2–10 mT) up to 70–100 mT (Mullender et al., 2016). In those samples where high-coercivity, low-blocking temperature minerals (i.e., goethite) were expected, a preheating to 150 °C was coupled to AF demagnetization. Stepwise TH demagnetization was carried out in laboratory-built furnaces, through 20–60 °C increments up to 340 °C (or until complete demagnetization). Magnetic remanence was measured after each demagnetization step on a 2G Enterprises SQUID magnetometer. Demagnetization diagrams were plotted as orthogonal vector diagrams (Zijderveld, 1967), and the characteristic remanent magnetizations (ChRMs) were isolated via principal component analysis (Kirschvink, 1980). Zijderveld diagrams from both TH and AF demagnetizations were filtered to distinguish overprint and provide more precise average declinations (Figure 3). Demagnetization paths with a mean angular deviation (MAD) value above 15° are removed because they are either totally chaotic (Figure 3a) or show too much scatter to give relatively precise directions (Figures 3b and 3c). Site mean directions were evaluated using a Fisher statistics (Fisher, 1953) of virtual geomagnetic poles (VGPs) corresponding to the isolated ChRMs (Figures 4 and 5). Here the N-dependent reliability envelope of Deenen et al. (2011) was applied to assess the quality and reliability of the calculated mean ChRM directions. These criteria assess whether (i) the scatter of VGPs can be explained by paleosecular variation (PSV) of the geomagnetic field ($A95_{min} \leq A95 \leq A95_{max}$), (ii) an additional source of scatter ($A95 > A95_{max}$) is present besides PSV, or (iii) the scatter underrepresents PSV, which may indicate acquisition of the magnetization in a time period too brief to fully sample PSV, for example, due to remagnetization or inappropriate sampling. We applied a fixed 45° cutoff (Johnson et al., 2008) to the VGP distributions of each site.

All sites are characterized by an internally homogeneous bedding attitude, thus excluding the possibility of applying a fold test (McFadden, 1990) at the site level, as the statistical parameters are identical before and after bedding correction. Similarly, no multiple sites of coeval ages were sampled, denying a between-sites fold test. For statistical analysis, the paleomagnetic toolkit on paleomagnetism.org was used (Koymans et al., 2016).

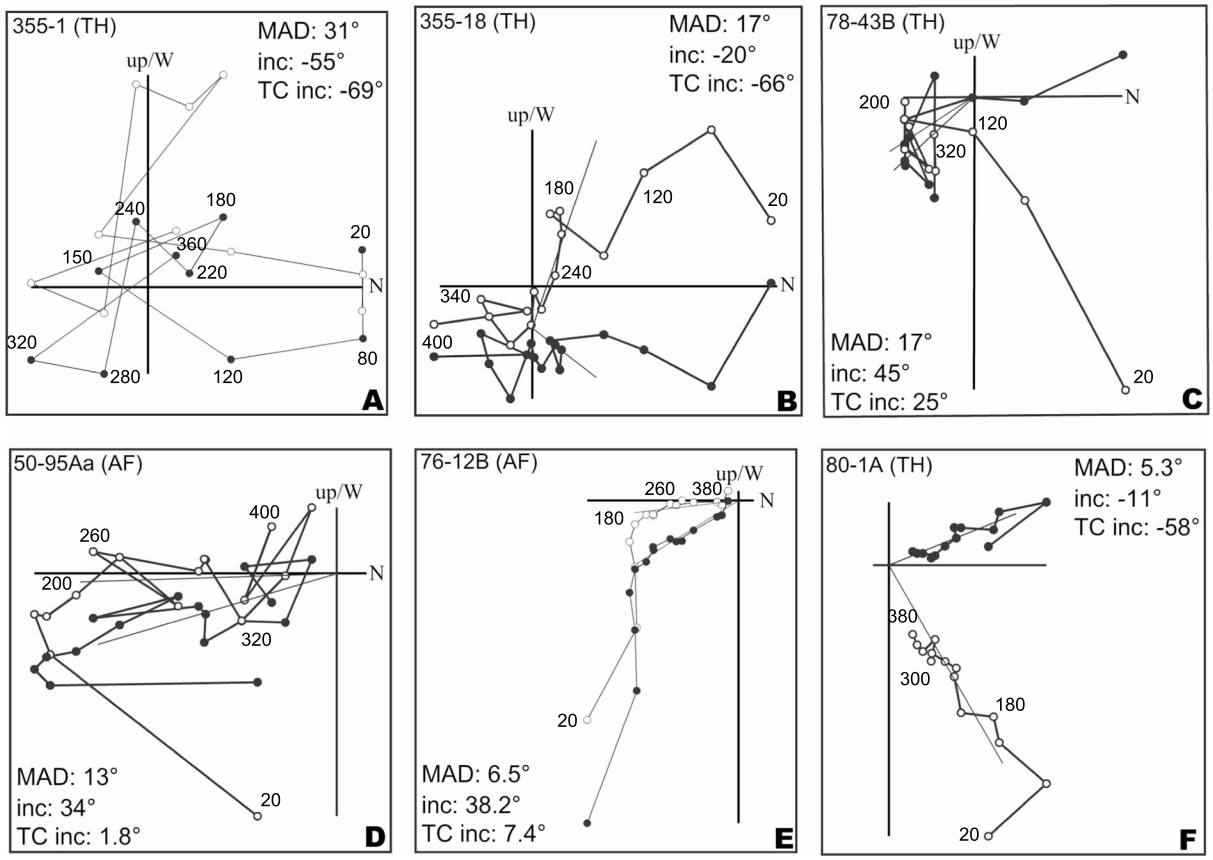

Figure 3. Orthogonal vector diagrams (Zijderveld, 1967) for representative specimens. Solid and open dots represent projection on the horizontal and vertical planes, respectively. Demagnetization step values are in milliTesla (alternating field demagnetization) or/and in degrees Celsius (thermal demagnetization). All vectors are shown after bedding tilt correction, with the nontilt-corrected inclinations, tilt-corrected inclinations, and the MAD values listed. (a) Kuaro River sample 355-1, (b) Kuaro River sample 355-18, (c) Samarinda Sungai Kunjang sample 78-43B, (d) Samarinda Stadion sample 50-95Aa, (e) Samarinda Batu Putih sample 76-12B, and (f) Samarinda sample 80-1A.

4.2. Site Descriptions

4.2.1. Kuaro River

In SE Kalimantan, the Kuaro River (Figure 6) exposes over 300 m of a shale dominated sequence underlain by metabasalt. The metabasalt is interpreted as part of an ophiolite of the Meratus Complex. Above this basalt, ~30 m of boulder and gravel conglomerate grades to sand and shale. The next 200+ m is mostly shale with thin sandstones. At the top of the exposure is a 1- to 2-m sandstone and a 1-m limestone, composed almost entirely of LBF. LBF collected from the limestone give an age range of latest Bartonian to Priabonian (Late Eocene) based on the presence of *Discocyclina* and *Nummulites* genera. Twenty-five samples were taken in shale, sandstone, and limestone exposed along the Kuaro river. The bedrock here has a strike/dip of 018/24.

The interpreted ChRMs of the Kuaro section are all of normal polarity. Inclinations before tilt correction are generally steeper than expected from the present-day location, which suggests that the samples have a primary magnetization. Sixteen samples yielded a tilt-corrected mean ChRM of D = 351.2 ± 6.5°, I = −8.8 ± 12.7° (Figure 4d and Table 1).

4.2.2. Berau Coal Mine

Berau Coal Mine (Figure 6) exposes silty shale, sandstone, and limestone. The base of the section is formed by limestone containing *Eulepidina* genus LBF indicative of Miocene-Oligocene and most likely Aquitanian age (V. Novak, personal communication, 2015). Further into the mine, shale and sandstone dominate. Exposures contain the LBF *Flosculinella* (Lower Burdigalian) and *Nephrolepidina ferreroi* (Burdigalian). Sampling took place at two exposures of Burdigalian rocks. Six samples were taken from the first exposure, which

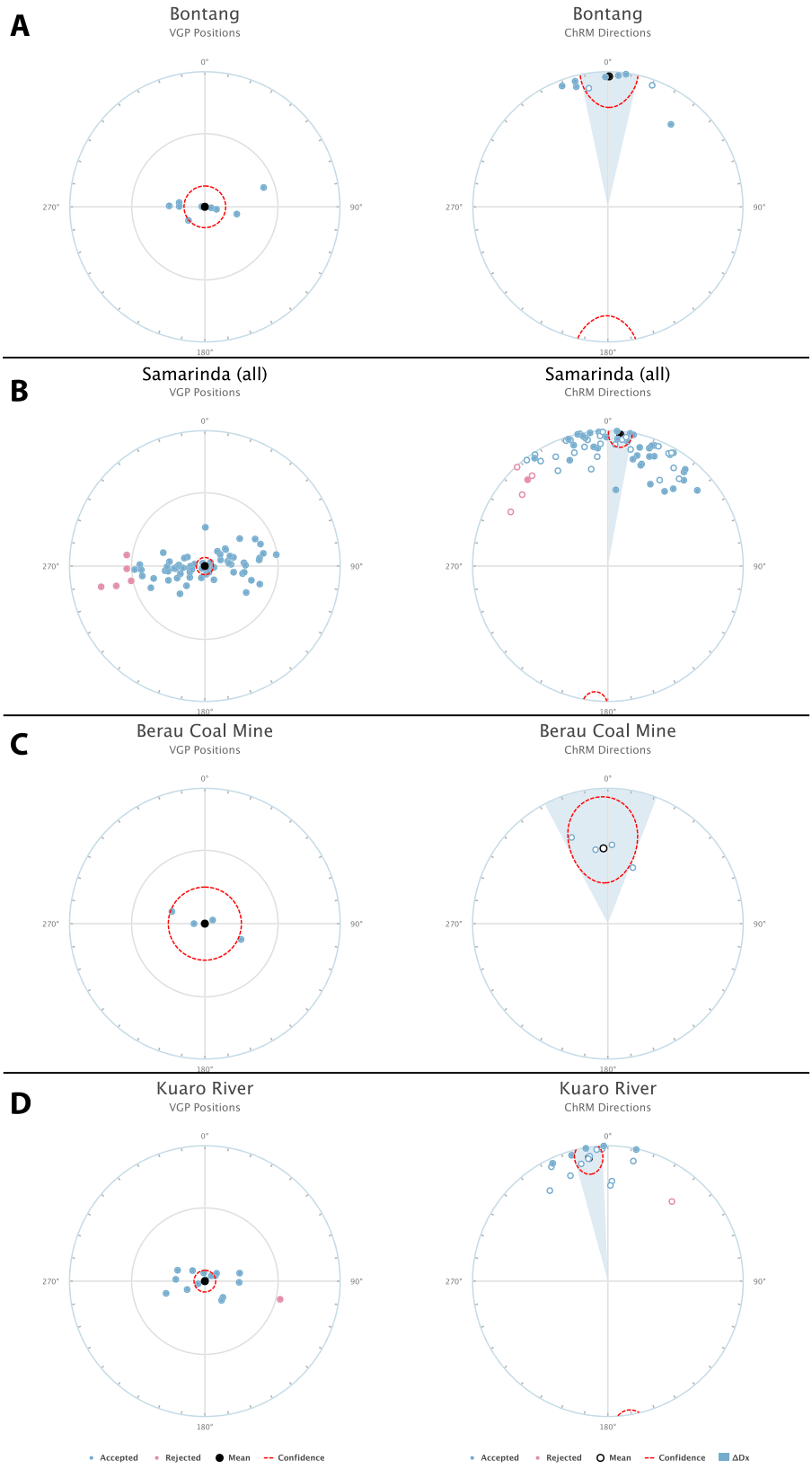

Figure 4. Equal area projections of paleomagnetic directions per site through the stratigraphy of the Kutai Basin. (a) Tortonian (Bontang), (b) Langhian-Serravalian (Samarinda), (c) Burdigalian (Berau coal mine) and (d) Bartonian-Priabonian (Kuaro River).

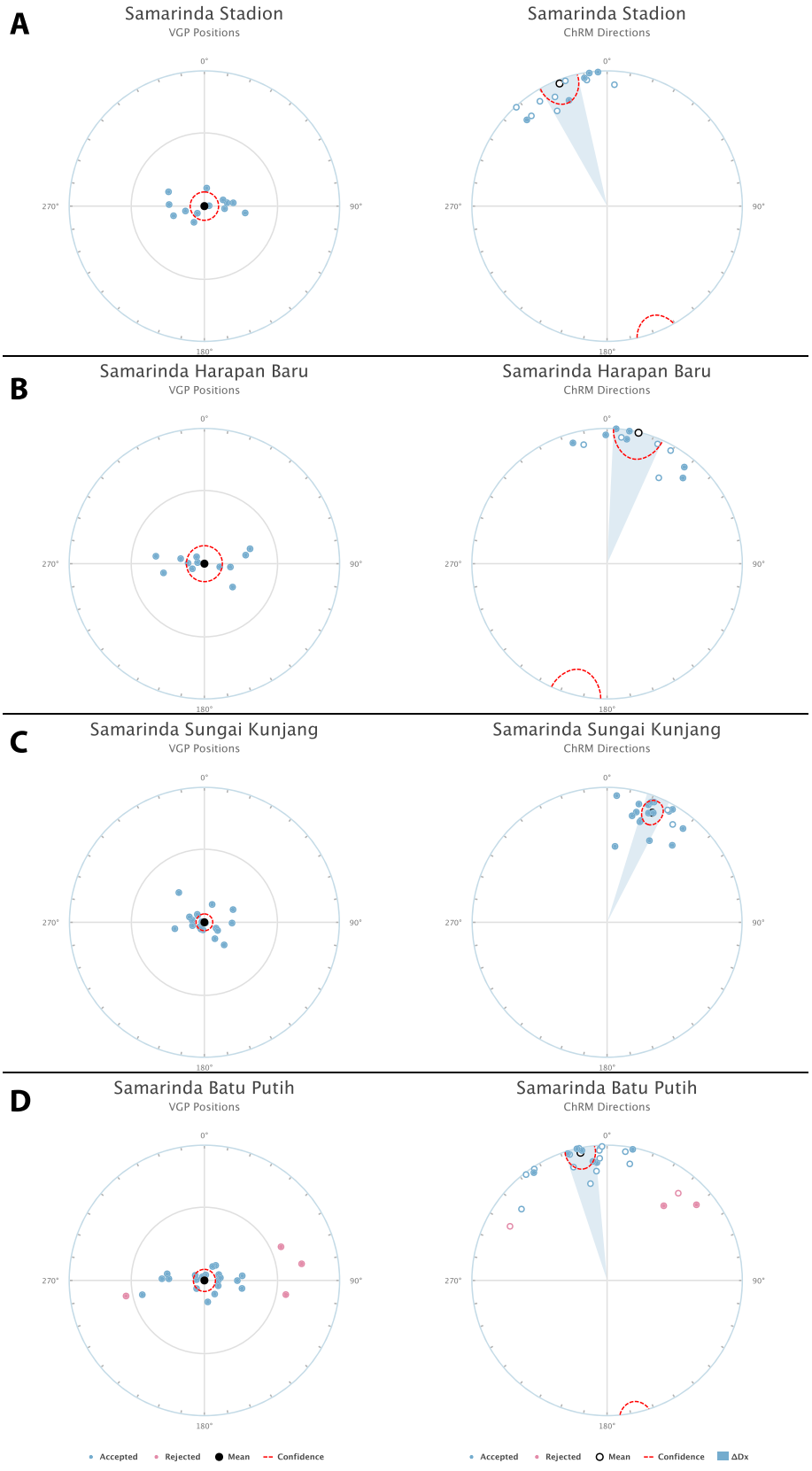

Figure 5. Equal area projections of paleomagnetic directions of subsites of the Miocene Samarinda section. (a) Stadion, (b) Harapan Baru, (c) Sungai Kunjang, and (d) Batu Putih.

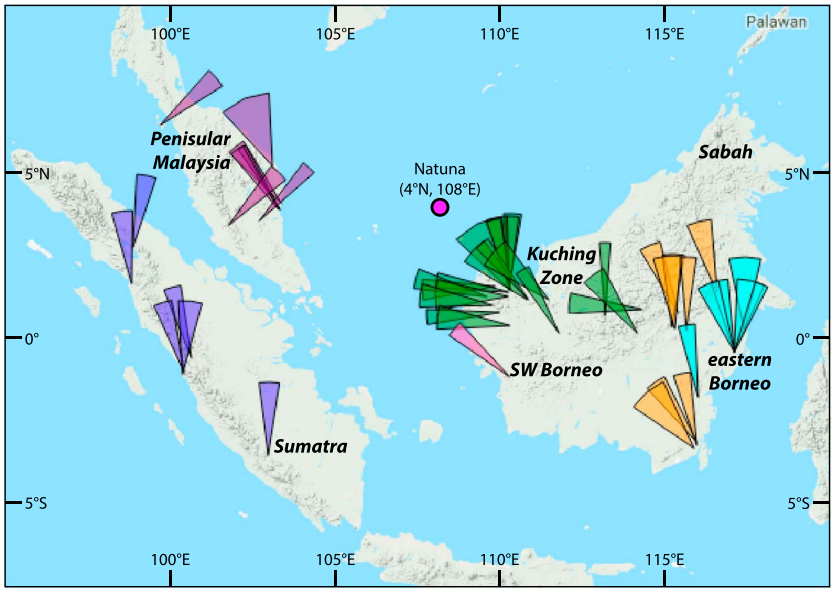

Figure 6. Maps with locations and declinations of paleomagnetic sites after applying compilation criteria, color-coded by region. Blue = Sumatra; purple = Peninsular Malaysia; green = Kuching zone; pink = SW Borneo (Schwaner Mountains); orange = Eastern Borneo; cyan = Eastern Borneo (this study).

contained ~25 m of interbedded brown shale, sandstone, and lignitic coal and has a strike/dip of 220/12. Six more samples were taken from a limb of a small plunging antiform of interbedded thin sandstones and shale with a strike and dip of 260/45.

The samples from Site A of the Berau Coal Mine were all ubiquitously weak, hundreds of microAmpère per meter, and showed mainly low-temperature components that indicated secondary magnetizations. At the shallow dipping (220/12) Site B, only four samples show a primary component, with a tilt-corrected mean ChRM of D = 356.7 ± 24.5°, I = 28.3 ± 28.3° (Figure 4c and Table 1).

4.2.3. Samarinda

Around the city of Samarinda (Figure 6), urban development has exposed over 4 km of Middle Miocene shelf to fluvial/deltaic sediments. The succession has been split into four continuous subsections, established by changes in paleoenvironment and unexposed intervals: Batu Putih (slope to shelf-edge patch reef), Sungai Kunjang (delta), Harapan Baru (delta to fluvial), and Stadion (transgression and return of deltaic/fluvial). Integrated biostratigraphy and magnetostratigraphy constrains the age range to ~17–11 Ma (Marshall et al., 2015). Over 400 samples were taken throughout the exposed stratigraphy. The strike/dip of bedrock changes throughout the section: Batu Putih = 024/61, Sungai Kunjang = 026/55, Harapan Baru = 032/55, and Stadion = 040/54.

From the 400 samples from Samarinda 60 samples passed the filters mentioned above. Results of the individual subsections show an apparent oscillation of the interpreted ChRM over time (Figure 5 and Table 1). For the calculation of the Apparent Polar Wander Path (APWP) of Borneo for the Cenozoic (see next section) we use these site averages following procedures in, for example, Torsvik et al. (2012). Combining all individual sample directions shows a strongly elongated data distribution that is unlikely to entirely result from the combination of PSV and inclination flattening, suggesting that some minor local rotation differences between these sites may have occurred. On average, the Samarinda locality yields a tilt-corrected mean ChRM of D = 005.4 ± 5.1°, I = 2.8 ± 10.3° (Figure 4b), showing that no significant rotation has occurred in the Samarinda area since ~17 Ma.

4.2.4. Bontang

The region around the town of Bontang (Figure 6) is dotted with small exposures in construction sites and small quarrying operations. Exposures range in stratigraphic thickness from a couple meters to ~30 m and reveal shelf to circumdeltaic shale, sand, and coaly beds with interspersing patch reefs of early Tortonian age (Renema et al., 2015). Sixteen samples were taken from a construction site on a patch-reef ridge

exposing tens of meters of shale. Structural trends are similar to Samarinda, showing a NNE uplift trend related to inversion of older rift faulting. The bedrock strike/dip is 080/20.

Samples of the Bontang sites were mostly very weak, with the ostensible original remanent magnetism occurring often at less than 100 μAm^{-1} of magnetic moment. The low dip of the bedding, normal polarity, and seeming lack of a differentiable low-temperature component, made these samples difficult to differentiate against modern overprint and an original signal, but the best diagrams showed a marked rise in inclination without tectonic correction, indicating that the orientation used is less likely to be an overprint. The mean ChRM is $D = 0.5° \pm 12.5°$, $I = 3.9° \pm 24.9°$ (Figure 4a and Table 1).

5. Paleomagnetic Data Compilation

The aim of our paper is to critically reassess the paleomagnetic constraints on the rotation history of SE Asia in the Cenozoic. In this section, we compiled a data set from paleomagnetic from Sundaland and Borneo, whereby we also included data from Mesozoic rocks, which will in part be used in our assessment of the Cenozoic history and in part may be used in future reconstructions back to older time. For this compilation, we adopted commonly used paleomagnetic reliability criteria summarized in, for example, Lippert et al. (2014) and Li et al. (2017): Data were not included if (1) sites were (likely) remagnetized or otherwise unreliable according to the original authors if reasons were given; (2) sedimentary sites consisted of less than five samples or volcanic localities consisted of less than five lava sites, distributed over a small area with lavas of similar age. Volcanic sites from single lavas should represent spot readings of the geomagnetic field where within-site scatter only results from (small) measuring errors. Therefore, we apply the widely used (e.g., Biggin et al., 2008; Johnson et al., 2008) cutoff of Fisher (1953) precision parameter $k < 50$ for individual lava sites. In the case of volcanic sites, it was often unclear whether a reported average was based on samples from one or more lavas. Where unclear, we consider every site from volcanic rocks a lava site and applied the strict reliability criteria that apply to those. Almost all lava sites in the study area were sampled in isolation, and most of these were thus discarded; (3) sedimentary or intrusion sites (where each sample may be considered a spot reading of the paleomagnetic field) or locality averages with at least five lavas (where each lava site represents a spot reading of the paleomagnetic field) yielded an $A95$ smaller than $A95_{min}$ in the sense of Deenen et al. (2011), since this suggests insufficient sampling of PSV, but may rather represent spot readings instead. In some cases, subdued $A95$ values may be caused by very slow sedimentation (Deenen et al., 2011), for example, for radiolarian cherts: our criterion is thus a conservative measure; (4) sedimentary or intrusion sites or locality averages with at least four lavas yielded an $A95$ larger than $A95_{max}$ in the sense of Deenen et al. (2011), which suggests that the scatter within the sites cannot be explained by PSV alone and other sources of scatter (e.g., local within-site rotations) must pertain. Since some of the available paleomagnetic data are derived from Cretaceous rocks deposited during the Cretaceous normal superchron, the presence of reversals, which is often used as criterion (e.g., Van der Voo, 1990), is not a general requirement. Remagnetized directions with precise age constraints on magnetization acquisition, and anomalous directions due to local tectonics, as pointed out by the original authors, are presented for reference but not included in the final discussion (e.g., Otofuji et al., 2017; Richter et al., 1999; Schmidtke et al., 1990).

Where available, we compiled paleomagnetic data based on the original specimen directions. Where these data were not available, we compiled the data by parametric sampling using paleomagnetism.org (Koymans et al., 2016). Declinations and inclinations were calculated relative to reference location 4°N, 108°E (Natuna; Figures 6 and 7). The compilation of paleomagnetic data is provided in Table 2, and data files compatible with www.paleomagnetism.org are provided in the supporting information.

Age constraints on rocks sampled for paleomagnetism in Sundaland and Borneo are poor. Igneous rocks sampled for paleomagnetism were seldom directly dated by the original authors but assigned an age based on lithostratigraphic correlations or ages assigned on geological maps. Where radiometric ages are available, these are often K-Ar ages, and the errors are not always provided. Most paleomagnetic studies only report the age of the sampled sedimentary rocks at system level for the Mesozoic or series level for the Cenozoic. In the absence of reliable age estimates, paleomagnetic data were excluded from this compilation. In recent years, however, age ranges of the sedimentary sequences have become better constrained by new biostratigraphic studies (e.g., Renema et al., 2015; Witts et al., 2012), and igneous rocks have been dated by modern radiometric methods, including the SHRIMP and laser ablation inductively coupled plasma mass spectrometer

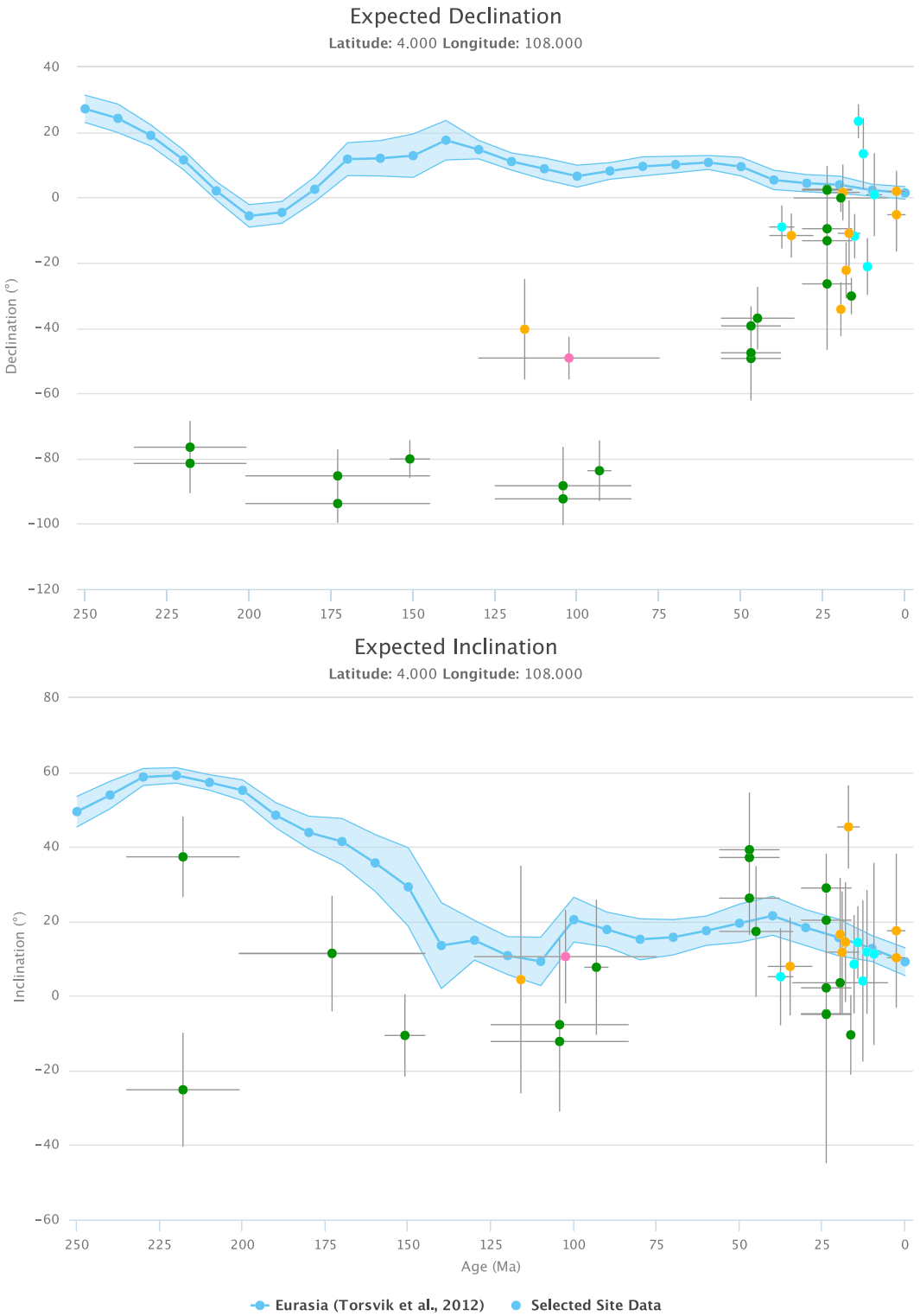

Figure 7. Compiled paleomagnetic data from Borneo compared to expected directions from the Apparent Polar Wander Path of Eurasia (Torsvik et al., 2012) calculated to reference location 4°N, 108°E (Natuna).

Tectonics

10.1029/2018TC005010

Table 2
Compilation of Paleomagnetic Data From Sundaland and Borneo After Application of the Reliability Criteria Formulated in This Paper

Site name	Lithology	Age	Minimum age	Maximum age	Latitude	Longitude	N	N_{45}	D	ΔD_x	I	ΔI_x	K	A95	$A95_{min}$	$A95_{max}$	Author
Peninsular Malaysia																	
Genting Sempah	Intrusion	218	201	235	3.350	101.830	22	22	43.8	7.7	48.8	7.7	22.4	6.7	3.5	11.7	Richter et al. (1999)
Gunong Raya	Intrusion	218	201	235	6.370	99.780	7	7	50.0	7.9	62.9	4.6	114.4	5.7	5.5	24.1	Richter et al. (1999)
Kuala Tahan road section	Sediment	132	100	164	4.230	102.400	67	61	68.1	6.3	18.4	11.4	9.6	6.2	2.3	6.2	Otofuji et al. (2017)
Kuala Wau section	Sediment	132	100	164	3.480	102.780	79	74	43.1	5.5	38.9	7.2	11.3	5.1	2.1	5.4	Otofuji et al. (2017)
Kuantan Dykes (Hayle)	Intrusion	104	79	129	3.800	103.370	80	80	328.6	3.1	41.6	3.8	32.7	2.8	2.1	5.2	Haile et al. (1983)
Kuantan SM88-19/EM91-7/8	Intrusion	104	79	129	3.980	103.410	21	21	321.7	6.9	6.7	13.7	22.1	6.9	3.6	12.0	Richter et al. (1999)
Kuantan SM86-2/3	Intrusion	104	79	129	3.820	103.320	26	26	325.2	5.5	38.1	7.3	31.8	5.1	3.3	10.5	Richter et al. (1999)
Kuantan SM88-21(A)	Intrusion	104	79	129	5.140	103.150	7	7	337.3	19.9	39.3	25.7	11.8	18.4	5.5	24.1	Richter et al. (1999)
Sumatra																	
PA2[a]	Sediment	132	100	164	−1.096	100.475	18	18	343.1	7.1	20.2	12.8	25.3	7.0	3.8	13.3	Advokaat et al. (2018)
ID154	Sediment	61	56	66	1.578	98.911	9	9	352.5	8.1	40.5	10.1	49.3	7.4	5.0	20.5	Sasajima et al. (1978)
ID166	Sediment	44.5	23	66	−1.149	100.433	10	10	6.4	9.3	−43.8	10.7	34.4	8.4	4.8	19.2	Sasajima et al. (1978)
ID163	Sediment	19.6	5.3	33.9	−0.642	100.718	9	9	345.0	6.7	−16.8	12.4	61.3	6.6	5.0	20.5	Sasajima et al. (1978)
ID132	Intrusion	13.8	10.8	16.8	2.692	98.930	8	8	10.9	7.6	9.2	14.9	54.1	7.6	5.2	22.1	Sasajima et al. (1978)
ID177	Sediment	12.8	2.6	23	−3.593	103.005	11	11	1.0	7.8	−24.5	13.3	36.9	7.6	4.6	18.1	Sasajima et al. (1978)
Borneo																	
Kuching Zone																	
Suti Semarang	Sediment	218	201	235	0.900	109.800	21	18	277.9	9.1	−28.9	14.5	16.5	8.8	3.8	13.3	Sunata and Wahyono (1987)
Gunung Bawan	Sediment	218	201	235	1.200	109.600	30	29	284.4	7.8	34.0	11.3	14.1	7.4	3.1	9.8	Sunata and Wahyono (1987)
Tengume	Sediment	173	145	201	0.700	110.000	40	39	266.6	5.8	7.9	11.3	16.8	5.8	2.8	8.2	Wahyono and Sunata (1987)
Tiong Cihan	Sediment	173	145	201	0.800	114.300	39	35	275.1	7.9	−1.6	15.8	10.4	7.9	2.9	8.7	Wahyono and Sunata (1987)
Penrissen (SR88-23)	Sediment	151	145	157	1.300	110.280	8	8	279.7	5.7	−15.8	10.6	98.7	5.6	5.2	22.1	Schmidtke et al. (1990)
Pedawan (SR88-20)	Sediment	104.3	83.6	125	1.180	110.280	8	8	271.5	11.8	−12.3	22.7	23.2	11.8	5.2	22.1	Schmidtke et al. (1990)
Lundu (SR88-14)	Sediment	104.3	83.6	125	1.500	109.900	15	15	267.4	7.9	−15.6	14.9	24.6	7.9	4.1	14.9	Schmidtke et al. (1990)
Dusun Bunut Quarry	Intrusion	93.2	89.7	96.7	0.300	110.300	6	6	276.5	9.1	2.3	18.2	55.0	9.1	5.9	26.5	Fuller et al. (1999)
Simunjam (SR88-2)	Sediment	47	38	56	1.100	110.850	6	6	312.6	11.1	33.2	16.4	41.2	10.6	5.9	26.5	Schmidtke et al. (1990)
Simunjam (SR88-4)	Sediment	47	38	56	1.080	110.900	7	7	320.7	5.8	18.9	10.5	112.8	5.7	5.5	24.1	Schmidtke et al. (1990)
Batang Undup (SR88-5)	Sediment	47	38	56	1.100	111.500	9	9	310.8	12.4	30.1	19.3	19.7	11.9	5.0	20.5	Schmidtke et al. (1990)
Kalasin	Sediment	45	33.9	56	0.100	114.200	27	20	323.0	9.3	4.0	18.6	13.2	9.3	3.6	12.4	Wahyono and Sunata (1987)

Tectonics

10.1029/2018TC005010

Table 2 *(continued)*

Site name	Lithology	Age	Minimum age	Maximum age	Latitude	Longitude	N	N_{45}	D	ΔD_x	I	ΔI_x	K	$A95$	$A95_{min}$	$A95_{max}$	Author
Kuching Quarry (SR85-9)	Intrusion	23.8	16.3	31.3	1.380	110.300	8	8	2.3	5.3	−2.9	10.5	111.2	5.3	5.2	22.1	Schmidtke et al. (1990)
Jalan Rock (SR86-26)	Intrusion	23.8	16.3	31.3	1.500	110.320	6	6	2.8	7.0	−9.7	13.6	94.0	6.9	5.9	26.5	Schmidtke et al. (1990)
Hua Sun Quarry (SR85-8)	Intrusion	23.8	16.3	31.3	1.360	110.380	10	10	346.4	5.7	23.6	9.7	77.4	5.5	4.8	19.2	Schmidtke et al. (1990)
Semengo Quarry (SR85-7)	Intrusion	23.8	16.3	31.3	1.390	110.310	8	8	350.2	8.0	14.8	15.1	49.5	8.0	5.2	22.1	Schmidtke et al. (1990)
Mr. Choo's (Haile2)	Intrusion	23.8	16.3	31.3	1.390	110.310	5	5	333.7	20.2	−11.4	39.0	15.5	20.1	6.3	29.7	Schmidtke et al. (1990)
Nanga Raun	Intrusion	19.6	5.3	33.9	0.600	113.200	22	22	0.0	4.2	−3.3	8.4	55.8	4.2	3.5	11.7	Sunata et al (1987)
Bukit Gembah	Intrusion	16.4	15.8	17	0.100	111.800	10	10	330.1	5.5	−20.4	9.8	80.5	5.4	4.8	19.2	Fuller et al. (1999)
SW Borneo																	
Schwaner Mountains[a]	Intrusion	102.5	75	130	−1.250	110.300	39	39	310.9	6.4	0.3	12.7	14.0	6.4	2.8	8.2	Haile et al. (1977)
Eastern Borneo																	
Batulicin	Intrusion	116	116	116	−3.400	115.900	5	5	319.7	15.4	−16.7	28.6	26.1	15.3	6.3	29.7	Sunata and Permanadewi (1998)
Kuaro River[a]	Sediment	37.6	33.9	41.3	−1.848	116.053	17	16	351.2	6.5	−8.8	12.7	33.4	6.5	4.0	14.3	This study
Tanjung	Sediment	34.7	28.1	41.3	−3.300	116.000	7	7	348.4	6.6	−9.5	12.9	84.8	6.6	5.5	24.1	Sunata and Permanadewi (1998)
Gunung Kukusan	Intrusion	19.6	18.84	20.34	−3.200	116.000	5	5	325.6	8.0	−4.1	16.0	92.1	8.0	6.3	29.7	Sunata and Permanadewi (1998)
Nakan[a]	Volcanic	19	14	24	0.250	115.250	7	7	1.2	8.3	4.7	16.6	53.3	8.3	5.5	24.1	Lumadyo et al. (1993)
Long Bagun	Intrusion	18	18	18	0.690	115.400	6	6	337.5	8.4	2.9	16.7	65.2	8.4	5.9	26.5	Fuller et al. (1999)
Telen River microgranite	Intrusion	17.1	13.8	20.4	1.300	116.600	6	6	345.8	9.6	39.4	12.4	57.8	8.9	5.9	26.5	Moss et al. (1997)
Samarinda Batu Putih[a]	Sediment	15.4	14.5	16.3	−0.500	117.140	25	21	348.2	6.6	−4.0	13.2	24.0	6.6	3.6	12.0	This study
Samarinda Sungai Kunjang[a]	Sediment	14.25	13.5	15	−0.500	117.140	19	19	22.4	5.1	13.2	9.7	45.5	5.0	3.7	12.8	This study
Samarinda Harapan Baru[a]	Sediment	12.75	12	13.5	−0.500	117.140	12	12	13.5	10.8	−0.5	21.6	17.2	10.8	4.4	17.1	This study
Samarinda Stadion[a]	Sediment	11.5	11	12	−0.500	117.140	13	13	338.8	8.5	−3.1	17.0	24.7	8.5	4.3	16.3	This study
Bontang[a]	Sediment	9.4	7.2	11.7	0.161	117.434	9	9	0.5	12.5	3.9	24.9	17.9	12.5	5.0	20.5	This study
Bigung[a]	Volcanic	2.655	0.01	5.3	0.170	115.660	5	5	354.2	11.0	8.8	21.6	49.3	11.0	6.3	29.7	Lumadyo et al. (1993)
Kelian[a]	Volcanic	2.655	0.01	5.3	0.200	115.340	6	6	1.7	6.1	3.1	12.2	120.9	6.1	5.9	26.5	Lumadyo et al. (1993)

Note. For a full list of reported paleomagnetic sites, see supporting information.
[a]Statistical paramaters were calculated on their original specimen directions; all other sites were parametrically sampled.

(LA-ICP-MS) U-Pb method on zircon and the $^{40}Ar/^{39}Ar$ method on white mica (e.g., Breitfeld et al., 2017; Davies et al., 2014; Setiawan et al., 2013). Where available, we have assigned these better-constrained ages to the paleomagnetic sampled rock units. We follow Gradstein et al. (2012) for the absolute ages of stratigraphic intervals.

5.1. Paleomagnetic Directions

5.1.1. Peninsular Malaysia

A wealth of paleomagnetic data are available from Mesozoic-Cenozoic rocks in Peninsular Malaysia (e.g., Haile, 1974; Haile et al., 1983; Haile & Khoo, 1980; McElhinny, 1974; Otofuji et al., 2017; Richter et al., 1999). Unfortunately, these data are subject to high age uncertainties due to highly discordant U-Pb ages (Liew & McCulloch, 1985; Liew & Page, 1985), resetting of the K-Ar system (Cottam et al., 2013; Krähenbuhl, 1991) and lack of biostratigraphy. Moreover, Peninsular Malaysia suffered widespread remagnetization (Otofuji et al., 2017; Richter et al., 1999). Reliable primary magnetizations, as concluded by the original authors, were only obtained from a handful of sites.

Paleomagnetic data for Peninsular Malaysia are almost all derived from Mesozoic rocks. We compiled paleomagnetic directions from Upper Triassic granites of the Main Range Batholith that were sampled at the Genting Sempah Pluton and the Gunong Raya Pluton (Richter et al., 1999). The majority of sites in the Upper Jurassic-Lower Cretaceous Tembeling Group did not pass a fold test and were interpreted as remagnetized (Otofuji et al., 2017; Richter et al., 1999). Only two road sections were considered to have primary directions (Otofuji et al., 2017). The sedimentary Kuala Tahun and Kuala Wau sections pass the Deenen et al. (2011) criteria and were included in the compilation. From the Cretaceous, a large paleomagnetic data set is available from the Kuantan Dykes (Haile et al., 1983; Richter et al., 1999). Finally, the Upper Cretaceous-Paleocene Segamat basalts were sampled at four closely spaced sites (Haile, 1974; Richter et al., 1999). It is unclear whether the sites reported by these authors represent averages of multiple lavas or individual lava sites, and the reliability and meaning of the results cannot be assessed. These results were discarded.

5.1.2. Sumatra

Three paleomagnetic studies have been conducted on Sumatra (Advokaat et al., 2018; Haile, 1979a; Sasajima et al., 1978). Advokaat et al. (2018) reported one site from Jurassic shales of the West Sumatran margin which passes the reliability criteria and shows northerly declinations. Sasajima et al. (1978) sampled Cenozoic volcanics, intrusions, and clastic sediments at 13 sites. Four sediment sites and one intrusive site yielded results that pass the reliability criteria and show declinations between 343° and 11° (Table 2). Haile (1979a) reported two sites, Geunteut and Breueh, and reported that these were derived from both intrusive sites as well as metavolcanics. Since these lithologies are unlikely to represent a synchronous geological formation, we did not incorporate these results.

5.1.3. Kuching Zone

Paleomagnetic directions from Mesozoic rocks of the Kuching Zone were compiled from eight sediment sites and one intrusion site. Site SR86-15 from the Upper Jurassic Penrissen Formation (Schmidtke et al., 1990) yielded an $A95 < A95_{min}$ and was discarded. The remaining seven Mesozoic sites show declinations of ~270° (Fuller et al., 1999; Schmidtke et al., 1990; Sunata & Wahyono, 1987; Wahyono & Sunata, 1987; Table 2). Eocene sediments were sampled at four sites and yielded declinations of ~315° (Schmidtke et al., 1990; Wahyono & Sunata, 1987). Two sites of Oligocene-Lower Miocene sediments, which were interpreted to belong to the top of the Silantek Formation, do not show significant declinations (Haile, 1979b). However, these two sites did not pass the Deenen et al. (2011) criteria and were therefore discarded. Schmidtke et al. (1990) suggested that they probably suffered remagnetization. Finally, we compiled paleomagnetic data from 12 sites of Oligocene-Miocene intrusions (Fuller et al., 1999; Schmidtke et al., 1990). Seven out of 12 sites did not pass the Deenen et al. (2011) criteria. The remaining five sites yielded declinations varying between 333° and 003°.

5.1.4. SW Borneo

Haile et al. (1977) sampled 41 Cretaceous magmatic and volcanic rocks from the Schwaner Mountains of SW Borneo for paleomagnetism and radiometric age dating. These igneous rocks yielded a wide spectrum of ages between 130 and 75 Ma (Davies et al., 2014; Haile et al., 1977). Only two samples on which paleomagnetic analyses were conducted were also dated, yielding K-Ar ages of 83.3 ± 1.9 Ma (K14B; biotite), 95.3 ± 3.0 Ma (K52; hornblende), and 89.0 ± 1.3 Ma (K52; biotite; Haile et al., 1977). Thirty-nine directions yielded an in situ mean ChRM of $D = 310.9° \pm 6.4°$, $I = 0.3° \pm 12.7°$, $K = 14.0$, $A95 = 6.4$.

5.1.5. Eastern Borneo: Meratus Complex and Kutai Basin

The 116 Ma Batulicin site in the Meratus Complex yielded a declination of 321.0° (Sunata & Wahyono, 1998), consistent with data from Cretaceous magmatic rocks in SW Borneo. Upper Eocene-Lower Oligocene sediments were sampled at two sites and yielded declinations of ~350° (Sunata & Wahyono, 1998; this study). Upper Eocene-Miocene rocks were sampled at five closely spaced sites along the Telen River (Fuller et al., 1999) near the Bengalon Fault Zone (Cloke et al., 1999; Moss, 1998). These five sites were key in the estimate of the amount and timing of rotation of Borneo in Fuller et al. (1999). Of these, the Telen River hbl-andesite site was undated, and an Oligo-Miocene age was assumed (i.e., >25 Myr uncertainty) and lacked paleohorizontal control. We therefore did not include this site in our compilation. A site from the Upper Eocene-Lower Oligocene Telen River turbidites and a site from an andesitic intrusion contained only four samples each and were discarded. A site with 15 samples at Mainyu was reported to be sampled from only three lavas (Fuller et al., 1999) and was therefore discarded.

Three sites where Upper Oligocene-Lower Miocene igneous rocks were sampled yielded declinations varying between 323° and 003° (Fuller et al., 1999; Lumadyo et al., 1993; Sunata & Permanadewi, 1998). Miocene sediments of the Kutai Basin were sampled at six sites, of which five passed the compilation criteria and showed tilt-corrected declinations between 338° and 022° (this study). Pliocene-Pleistocene basaltic lavas were sampled at three closely spaced sites (Lumadyo et al., 1993). One site did not pass the compilation criteria, and the other sites showed northerly declinations.

5.1.6. Sabah

Upper Valanginian-Barremian (Lower Cretaceous) radiolarian chert in Sabah yielded stable demagnetizations with a ChRM of $D = 278.6 \pm 4.3°$, $I = 0.2 \pm 8.5$, $K = 146.7$, $A95 = 4.3$, $n = 9$ (Fuller et al., 1991). We note that this site did not pass the Deenen et al. (2011) criteria as it shows $A95 < A95_{min}$. Therefore, we discarded this site.

Paleomagnetic data reported by Cullen et al. (2012) from the Upper Eocene-Lower Miocene Crocker Formation and the Lower Miocene Kudat Formation reveal CW as well as CCW rotations that may be local rotations related to complex deformation. Field observations (Cullen et al., 2012) show folded strata with plunging noncylindrical fold axes. In such cases, a more advanced tectonic correction is required (Pueyo et al., 2003). Furthermore, the data from Cullen et al. (2012) show a wide spread in inclinations from −84.5° to 48.7°, suggesting syndeformational remagnetization. Fuller et al. (1999) also identified that the Crocker Formation experienced remagnetization, as demonstrated by present-day field overprints. We therefore did not include paleomagnetic data from the Crocker and Kudat Formations in our compilation. Also, data from a 13.3 ± 5.3-Ma granodiorite from the Kapa Quarry near Mt. Kinebalu (Fuller et al., 1991, 1999; Schmidtke et al., 1985) did not pass the reliability criteria.

5.2. Summary of Paleomagnetic Results

We compiled and analyzed 79 reported paleomagnetic sites, including the seven new ones reported in this paper, from Sundaland and Borneo that were interpreted by the original authors to carry a primary magnetization. Of this data set, a total of 12 sites were discarded because they represent individual lava sites, three sites were discarded because $n < 5$, and 14 sites were discarded because $A95 < A95_{min}$ or $A95 > A95_{max}$ (Table S1). The resulting 48 sites (Table 2) are used for analysis below.

Eight sites (out of 14) from Peninsular Malaysia carried reliable paleomagnetic directions. Upper Triassic and Upper Jurassic-Lower Cretaceous rocks from Peninsular Malaysia show declinations of 043–050°, whereas Upper Cretaceous dykes show declinations of ~328° (Figure 6). Seven sites (out of 15) from Sumatra passed the compilation criteria and show declinations that indicate that Sumatra did not experience vertical axis rotations exceeding 11° CW or 17° CCW relative to the magnetic north since the Late Jurassic (Figure 6).

A total of 34 sites (out of 51) from Borneo passed the reliability criteria. Mesozoic sediment sites from the Kuching Zone show declinations of ~270° to ~280°, whereas Cretaceous magmatic rocks from the Schwaner Mountains and Meratus Complex show declinations of ~315° (Figures 6 and 7). Middle Eocene sediments from the Kuching Zone show declinations of ~315°, thus suggesting a ~45° CCW rotation of the Kuching Zone between the Late Cretaceous and Middle Eocene (e.g., Fuller et al., 1991, 1999; Schmidtke et al., 1990; Figure 7), which we do not reconstruct in further detail. Upper Eocene-Miocene sediment sites from eastern Borneo show declinations between 344° and 022°. Oligocene-Miocene igneous rocks from the Kuching Zone and eastern Borneo show declinations varying between 323° and 003° (Figure 8).

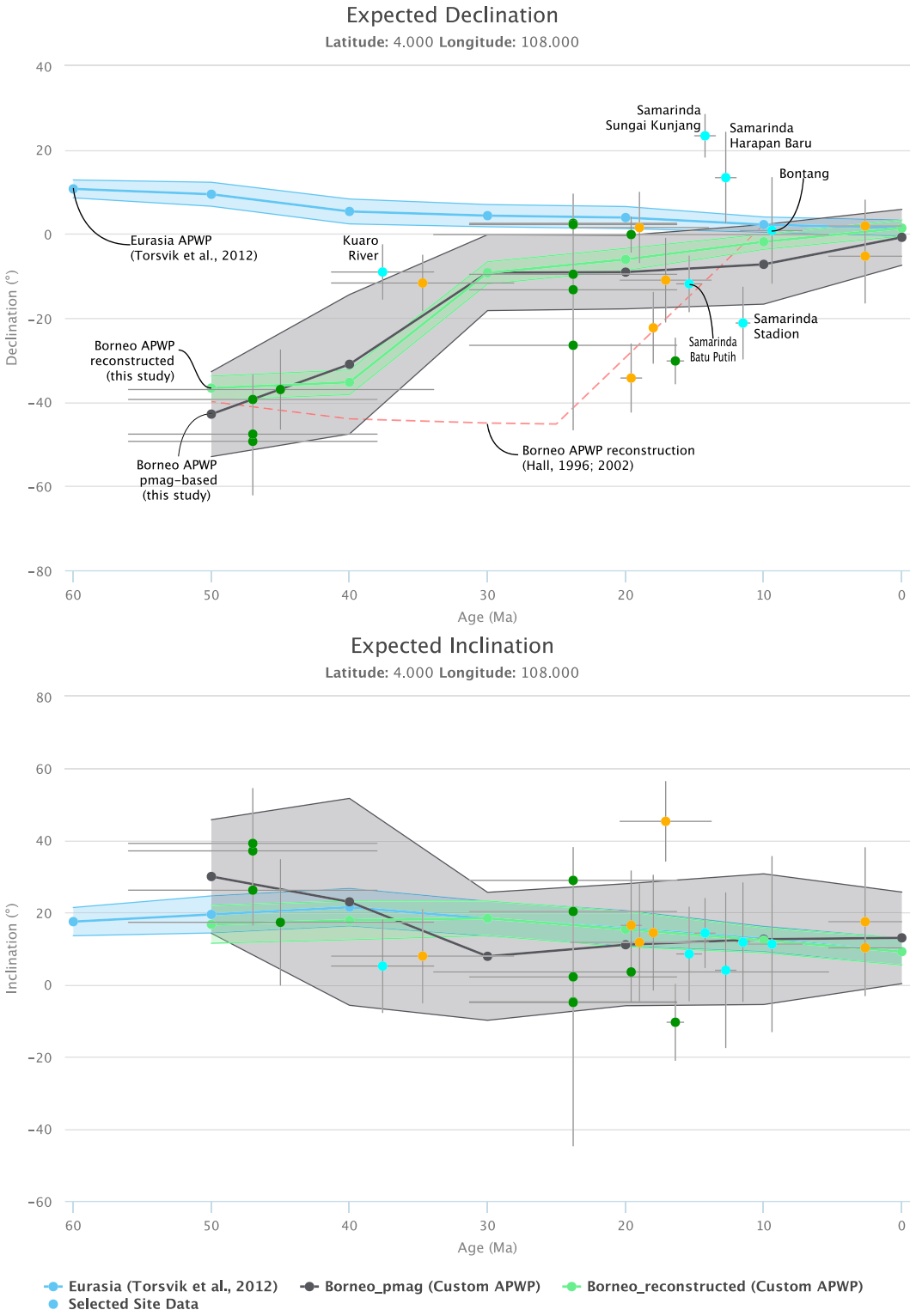

Figure 8. APWP of Eurasia (blue; Torsvik et al., 2012), paleomagnetic data-based APWP of Borneo (gray), and predicted APWP based on our reconstruction of the rotation of Borneo (light green), compared to paleomagnetic data from Borneo calculated to reference location 4°N, 108°E (Natuna). APWP = Apparent Polar Wander Path.

Table 3
Apparent Polar Wander Path Calculated for the Cenozoic of Borneo Based on the Data Compilation Listed in Table 2

Latitude	Longitude	A95	Age (Ma)
87.3	90.5	6.6	0
82.4	36.6	9.4	10
80.8	28.3	8.7	20
80.8	18.0	9.0	30
58.3	34.4	16.2	40
46.2	37.2	9.7	50

We calculated an APWP for Borneo based on paleomagnetic site averages from Cenozoic rocks, which suggests that Borneo underwent ~35° CCW rotation during the Late Eocene (41.2–33.9 Ma) and a further ~10° CCW rotation during the Miocene (Figure 8 and Table 3). The APWP is calculated from 50 to 0 Ma in 10-Myr intervals with a 20-Myr sliding window, similar to the procedures in Torsvik et al. (2012). The rotation history of Borneo that follows from the paleomagnetic sites that pass our reliability criteria is clearly different from that interpreted by Fuller et al. (1999), who suggested that the entire rotation occurred in Miocene time. This conclusion, however, was strongly biased by their a priori assumption that sites that yielded no significant declination from rocks older than 10 Ma were remagnetized. As a result, only sites that showed rotations were interpreted to be reliable, giving heavy weight to the rotated sites sampled in the Bengalon Fault Zone, most of which do not pass our reliability criteria because of low *n*, no paleohorizontal control, and/or absence of age constraints. Fuller et al. (1999) provided no rationale for this assumption and did not explore the possibility that rotations occurred earlier. As Cullen et al. (2012) already noted, Fuller et al. (1999) discarded data of Lumadyo et al. (1993) from Upper Eocene and Lower Miocene volcanics because these showed no significant declination. However, Lumadyo et al. (1993) reported that there was no petrographic or rock magnetic reason to assume a remagnetization, that the data passed the fold test (thus, magnetization was acquired prior to folding), and that folding was Middle Miocene in age. So even if there was a remagnetization event, this must have occurred prior to Middle Miocene folding and the samples would still record a component of CCW rotation. Evidently, the results of Lumadyo et al. (1993) do not record any component of rotation, and therefore, CCW rotation was thus already largely completed before the middle Miocene. We consider our APWP (Figure 8), which is based on a straightforward and objective analysis of the paleomagnetic constraints on Borneo's rotation using widely used independent reliability criteria, as a better basis for kinematic reconstruction of Borneo for the Cenozoic, which is outlined below.

6. Reconstruction

Our new reconstruction (Figure 9) aims to reconcile rotations in Borneo. We test our reconstruction against paleomagnetic data via the online platform paleomagnetism.org (Koymans et al., 2016), where we use a tool that allows to rotate the Global Apparent Polar Wander Path (GAPWaP) (Torsvik et al., 2012) into the coordinates of the reconstructed block if the Euler poles of this block are provided in 10-Myr intervals relative to South Africa (701), as described in Li et al. (2017). In our new reconstruction, rotations of Sundaland and Borneo were iteratively improved to become consistent with the paleomagnetic data (Figure 8) and structural constraints summarized above.

We use the GPlates free plate reconstruction software for our kinematic restoration (http://gplates.org; Boyden et al., 2011). Eurasia is reconstructed relative to South Africa using the Euler rotations of the global reconstruction of Seton et al. (2012), updated with Neogene North Atlantic reconstructions of DeMets et al. (2015). When comparing our reconstruction against paleomagnetic data, we use the paleomagnetic reference frame of Torsvik et al. (2012). When comparing our reconstruction against mantle structure, we use the global moving hot spot reference frame of Doubrovine et al. (2012). Small-scale motions of South China relative to Eurasia for the Neogene are reconstructed following Van Hinsbergen et al. (2011), based on Replumaz and Tapponnier (2003). The collision of India with Asia and deformation in Tibet are reconstructed according to van Hinsbergen et al. (2018). We use the paleomagnetically constrained deformation reconstruction of Indochina of Li et al. (2017), where the stable eastern part of Indochina rotates 15° CW relative to South China in the Oligocene-Early Miocene. Following constraints summarized in van Hinsbergen et al. (2011), we reconstruct 100-km sinistral displacement along the Mae Ping Fault and 100-km dextral displacement along the Three Pagodas Fault between 40 and 23 Ma.

6.1. Sundaland

We reconstruct Sundaland relative to Indochina. Following Watkinson et al. (2008, 2011) and Watkinson (2009), we reconstruct dextral displacements of 23 km on the Ranong Fault and 6 km on the Khlong Marui Fault at 88–81 Ma. We reconstruct dextral displacements of 113 km on the Ranong Fault and 31 km on the Khlong Marui Fault between 59 and 40 Ma. We reconstruct sinistral displacements of 66 km on the

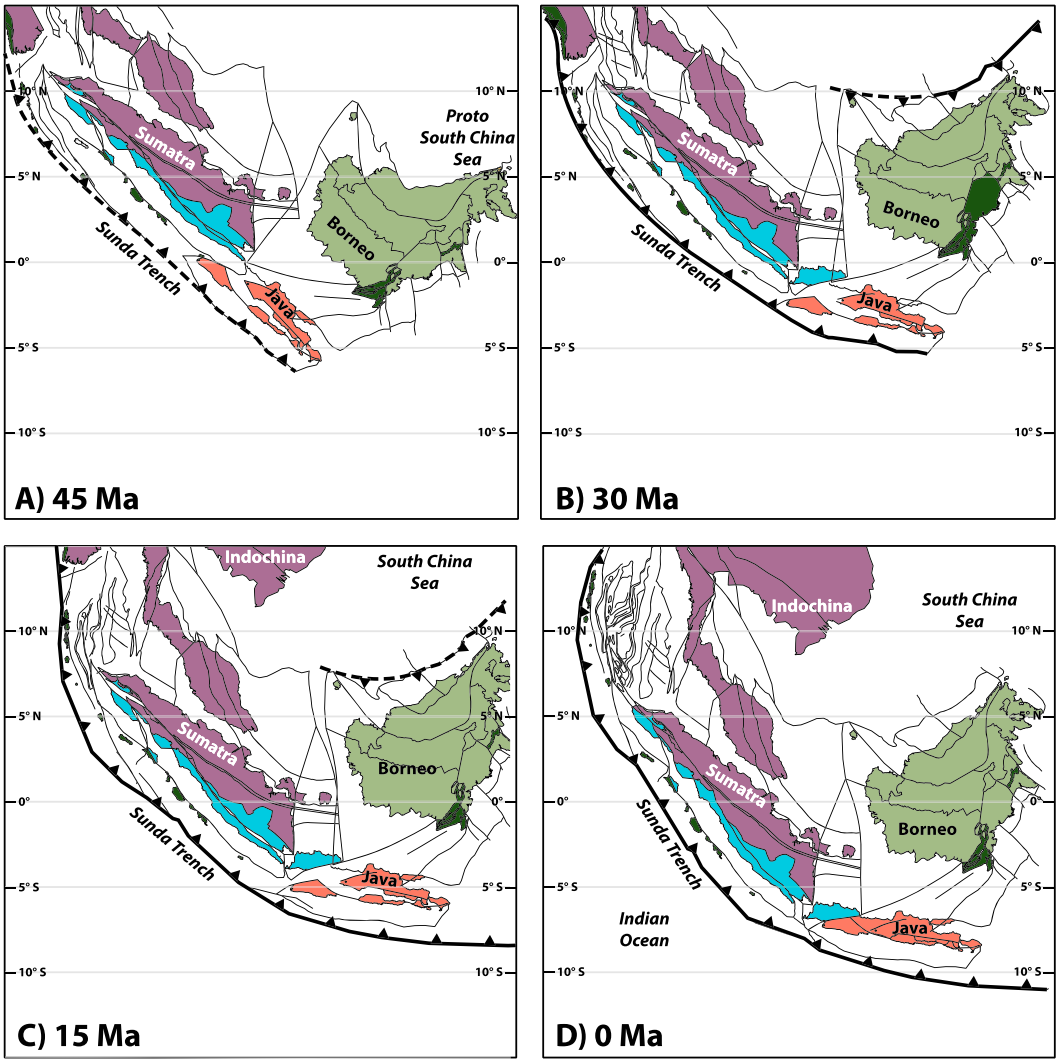

Figure 9. Time slices of our reconstruction in the paleomagnetic reference frame of Torsvik et al. (2012). (a) 45 Ma, (b) 30 Ma, (c) 15 Ma, and (d) 0 Ma.

Ranong Fault and 20 km of the Khlong Marui Fault between 38.3 and 22.6 Ma, based on $^{40}Ar/^{39}Ar$ biotite ages (Watkinson et al., 2011) and Rb/Sr mica—whole rock isochrons (Kanjanapayont, Klötzli, et al., 2012).

Compilation of paleomagnetic sites from the Thai Peninsula by Li et al. (2017) indicate ~15°CW Cenozoic rotation, similar to stable Indochina. The paleomagnetic sites in Sumatra show no significant declinations since the Late Jurassic. Conversely, paleomagnetic sites in Peninsular Malaysia show ~50° CCW rotation relative to Indochina since the Late Cretaceous. If we assume that this represents a coherent rigid block rotation of entire Sundaland and accommodate this rotation along the Songkla-Penang Fault, we obtain unrealistic large shortening amounts along this fault and at the Sunda Shelf. In addition, such a reconstruction would yield a Cenozoic Sunda trench with a N-S orientation, at high angles to the tomographically imaged Sunda Slab (Figure 2). We consider it therefore unlikely that the ~50° CCW rotation represents a regional rotation of Sundaland. Harun (2002) suggested that Peninsular Malaysia was deformed due to regionally distributed shear. We therefore consider the large (CCW) declinations observed in Mesozoic rocks from eastern Peninsular Malaysia to represent local rotations during Late Cretaceous extension and Late Eocene-Early Oligocene transpression (Ali et al., 2016; François et al., 2017; Harun, 2002).

In addition to paleomagnetic constraints from Sumatra on the regional rotation of Sundaland relative to Indochina, we also use tomographic constraints and align Sundaland throughout the Cenozoic with the orientation of the Sunda slab. Throughout the upper mantle and the upper part of the lower mantle, there

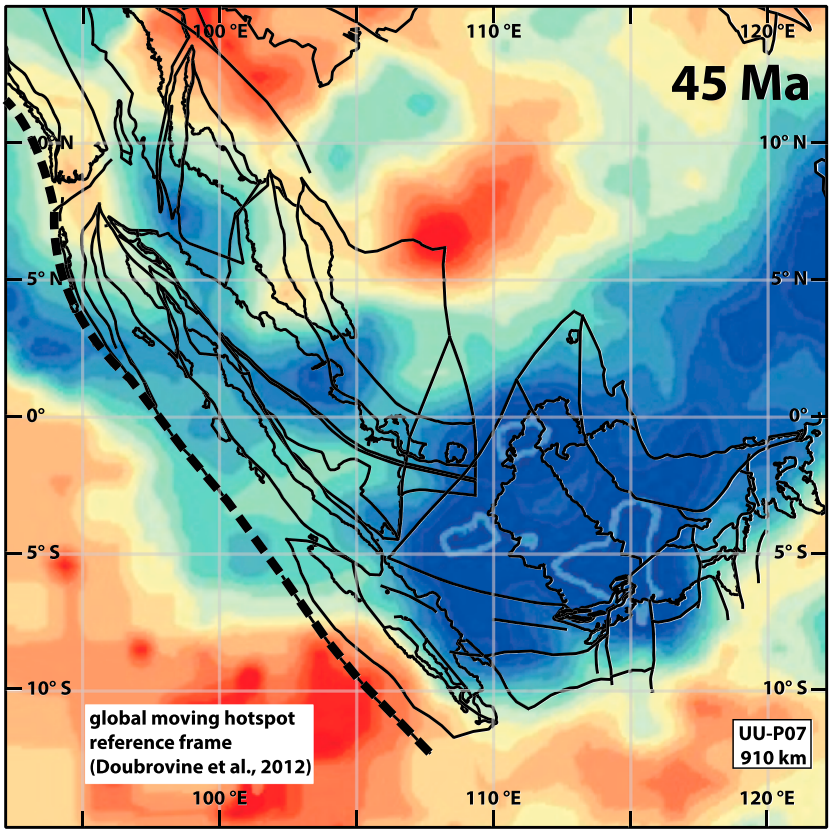

Figure 10. Reconstruction at 45 Ma in the global moving hot spot reference frame of Doubrovine et al. (2012), with a tomographic slice at 910 km depth of the UU-P07 model (Amaru, 2007; Hall & Spakman, 2015; van der Meer et al., 2017, available at www.atlas-of-the-underworld.org).

is no significant change in orientation of the Sunda Slab (Figure 2), and we therefore maintain Sundaland in its present-day orientation relative to the mantle since 45 Ma (Figure 10), although we do observe some small differences between the tomography and reconstructed orientation which may be explained by post-45-Ma deformation of the Sunda slab. Our reconstruction implies a ~15° CCW rotation of southern Sundaland (Sumatra and Peninsular Malaysia) relative to northern Sundaland (Thai Peninsula) and Indochina. Following Richter et al. (1999) we accommodate this 15° differential rotation along the Songkla-Penang Fault. This implies ~40-km extension in the North Sumatra Basin and ~35-km shortening along the Songkla-Penang Fault. It is likely that this differential rotation was distributed over a larger area in the Sunda Shelf.

6.2. Restoring Rotations in Borneo

We reconstruct Borneo relative to Sundaland. Based on geologic observations reviewed above, we consider Borneo as one coherent block since the Middle Eocene, consistent with earlier inferences (Hall, 1996, 2002; Hall et al., 2008). Based on the APWP that we calculated for Borneo, we reconstruct 35° CCW rotation in the Late Eocene (41.2–33.9 Ma). The paleomagnetic data suggest an additional 10° CCW rotation from the Early Miocene (23 Ma). We have chosen the rotation pole of Borneo such that it implies minimal extension in the West Java Sea and minimal shortening between Borneo and Malaysia. Our reconstruction then implies ~115-km E-W extension along N-S trending Late Eocene normal faults in the western Java Sea and ~320-km shortening between the NW tip of the Kuching Zone and eastern Sundaland. A comparison between the calculated APWP based on Borneo's paleomagnetic sites and the global APWP of Torsvik et al. (2012) in coordinates of Borneo according to our reconstruction is illustrated in Figure 8.

7. Discussion

We will now use our paleomagnetically consistent kinematic restoration above to evaluate previous models for the kinematic evolution of SE Asia and discuss possible geodynamic drivers for rotations in Borneo.

The data summarized and discussed above show that Borneo's Late Eocene ~35° CCW rotation requires extension in the West Java Sea, contraction in the northern Sunda Shelf, and convergence between Borneo and Indochina. Parts of this convergence may have been accommodated by deformation in the Malay Peninsula (Ali et al., 2016; François et al., 2017; Harun, 2002) and displacement along the Lupar Line. How and where else this deformation is accommodated remains difficult to demonstrate. For instance, despite the presence of very deep basins on the Sunda Shelf, which initiated in the Eocene, there is little evidence for major extension or shortening (Hall et al., 2008; Hall & Morley, 2004). Hall (2002) realized the same problem, even though his reconstruction based on then-available interpretations based on paleomagnetic data compiled by Fuller et al. (1999) assumed a 25- to 10-Ma rotation of Borneo, that is, younger than argued for in this paper. Hall (2002) solved the regional space problems by modeling the major SE Asian peninsulas and islands as separate rigid blocks that regionally distribute rotation and extension. We concur with Hall (2002) that the major net contraction and extension required by the rotation of Borneo relative to the remainder of Sundaland and Indochina is likely regionally distributed and its localized nature in our reconstruction is an artifact of modeling with rigid fragments (see also Hall, 2011, 2012). Better constraints on the magnitude and timing of extension, shortening, and strike-slip faulting in Sundaland are required to enable modeling of the region with deforming fragments. More paleomagnetic data, particularly in Sumatra east of the Sumatran Fault System, would allow reconciling the distribution of gradual or abrupt change in this Late Eocene rotation as a basis for a further refined kinematic restoration.

We may now explore what may have driven the rotation history of Borneo. Our new constraints showing that the ~35° CCW rotation occurred in the Late Eocene opens new possibilities for correlations to regional plate kinematic events hitherto not considered. Hall (2002), assuming the 25- to 10-Ma timing of rotation of Fuller et al. (1999), suggested that the Cenozoic Borneo rotation was driven by the Late Oligocene-Early Miocene collision of the Sula Spur promontory of the Australian Plate with eastern Sundaland. The minor, ~10° CCW rotation since the Early Miocene constrained in the APWP of Borneo (Figure 8) may indeed have been driven by this collision. Our new constraints showing a Late Eocene rotation coincide with two regional phenomena: (1) the onset of rapid northward motion of Australia relative to Eurasia around 45–40 Ma (Whittaker et al., 2007) and (2) the *Sarawak Orogeny* (Hutchison, 1996) or Rajang unconformity (Hall & Breitfeld, 2017) on NW Borneo, which involved folding and thrusting of the Upper Cretaceous-Upper Eocene turbidites of the Rajang Group (Figure 1) on NW Borneo. The deformed Rajang Group is separated by a regional unconformity of around 40–37 Ma (see discussion in Hall, 2012) from the overlying Upper Eocene-lowest Miocene Crocker Group showing timing of deformation (Van Hattum et al., 2013). Hutchison (1996) originally interpreted the Sarawak Orogeny to be caused by collision of a continental block with Kuching Zone, but Moss (1998) suggested that the last microcontinental arrivals at the Kuching Zone were as old as 80 Ma, after which subduction ceased and a remnant *proto-South China Sea* ocean remained between the Kuching Zone and South China. Hall (2012) therefore concluded that the Sarawak Orogeny was not caused by continental collision. Our new constraints showing a timing of rotation of Borneo coinciding with the Sarawak Orogeny leads us instead to interpret that the rotation is the result of partitioning of the inception of Australia-Eurasia convergence over (1) the new Sunda subduction zone below Java, where the oldest record of subduction is provided by volcanics with K-Ar whole rock ages of 37.55 ± 1.96 Ma (Soeria-Atmadja et al., 1994) and volcaniclastic sandstones with zircons that yielded SHRIMP U-Pb ages of ~42.7–41 Ma (Smyth et al., 2008), and (2) northward rotational motion of Borneo. This rotation of Borneo requires convergence with South China, and the Sarawak Orogeny may thus mark the onset of subduction of the proto-South China Sea below northern Borneo. This onset of subduction was followed by—and may have triggered—the opening of the South China Sea in Oligocene-Early Miocene time (Briais et al., 1993; Hall, 2002) and the rifting of blocks away from South China (e.g., Shao et al., 2017; Van Hattum et al., 2013) that eventually, in Miocene time, arrived at the North Borneo trench finalizing the modern architecture of the island (Hall et al., 2008).

8. Conclusions

In this study, we reviewed paleomagnetic constraints on Mesozoic-Cenozoic rotations in Sundaland and Borneo and provide new data from Eocene-Miocene sediments of Borneo to obtain new time constraints on these rotations. We built a new reconstruction of Cenozoic rotations in Sundaland and Borneo integrating paleomagnetic data with geologic observations and tested this reconstruction against mantle tomography to

assess whether paleomagnetic results from Sundaland may be representative of a regional coherent block rotation.

The main results and conclusions are the following:

1. We provide a thoroughly evaluated, updated paleomagnetic database for Sundaland (Peninsular Malaysia and Sumatra) and Borneo that passes a series of widely used quality criteria.
2. We demonstrate with paleomagnetic data and mantle tomography that the Sunda trench did not experience significant vertical axis rotations since the Late Jurassic.
3. Borneo underwent a ~35° CCW rotation in Late Eocene and an additional ~10° CCW rotation since the Early Miocene.
4. The Late Eocene rotation of Borneo coincides with an acceleration of northward motion of Australia relative to Eurasia. In the Late Eocene, convergence was predominantly accommodated by CCW rotation and northward motion of Borneo and Java, followed by orthogonal subduction below Java since the Oligocene. This rotation must have been associated with convergence between Borneo and Indochina, which we suggest was accommodated by inception of southward subduction of the proto-South China Sea below Borneo, recorded by the Sarawak Orogeny around 40–37 Ma.

Acknowledgments

E. L. A. and D. J. J. v. H. acknowledge funding through ERC Starting grant 306810 (SINK) to D. J. J. v. H. N. T. M. acknowledges funding by the Marie Curie Actions Plan, Seven Framework Programme (grant 237922). W. S. acknowledges support by the Research Council of Norway through its Centres of Excellence funding scheme, project 223272. All the paleomagnetic data used are listed in the references. We would like to thank the Indonesian geological survey for their assistance with logistics and fieldwork, Alexander Limbong and Robert Morley for help in the field, Mark Dekkers and the late Tom Mullender for their guidance in the laboratory and paleomagnetic discussion, Vibor Novak for foraminifera identification, Marco Maffione and Daniel Pastor-Galán for constructive criticism, and Ian Watkinson for discussions on the Ranong and Khlong Marui Faults. We appreciated constructive reviews by Anne Replumaz and Robert Hall.

References

Abdullah, N. T. (2009). Mesozoic stratigraphy, *Geol. Penins. Malaysia Kuala Lumpur, Univ. Malaya,* Geol. Soc. Malaysia, 87–132.

Advokaat, E. L., Bongers, M. L. M., Rudyawan, A., BouDagher-Fadel, M. K., Langereis, C. G., & Van Hinsbergen, D. J. J. (2018). Early Cretaceous origin of the Woyla Arc (Sumatra, Indonesia) on the Australian plate. *Earth and Planetary Science Letters*, *498*, 348–361. https://doi.org/10.1016/j.epsl.2018.07.001

Ali, M. A. M., Willingshofer, E., Matenco, L., Francois, T., Daanen, T. P., Ng, T. F., et al. (2016). Kinematics of post-orogenic extension and exhumation of the Taku Schist, NE Peninsular Malaysia. *Journal of Asian Earth Sciences*, *127*, 63–75. https://doi.org/10.1016/j.jseaes.2016.06.020

Amaru, M. L. (2007). Global travel time tomography with 3-D reference models

Asis, J., & Jasin, B. (2012). Aptian to Turonian Radiolaria from the Darvel Bay Ophiolite Complex, Kunak, Sabah. *Bulletin. Geological Society of Malaysia*, *58*, 89–96.

Barber, A. J., & Crow, M. J. (2005). Structure and structural history. *Geological Society, London, Memoirs*, *31*(1), 175–233. https://doi.org/10.1144/GSL.MEM.2005.031.01.13

Barber, A. J., & Crow, M. J. (2009). Structure of Sumatra and its implications for the tectonic assembly of Southeast Asia and the destruction of Paleotethys. *Island Arc*, *18*(1), 3–20. https://doi.org/10.1111/j.1440-1738.2008.00631.x

Barber, A. J., Crow, M. J., & Milsom, J. (2005). *Sumatra: Geology, resources and tectonic evolution*. London: Geological Society of London.

Ben-Avraham, Z., & Emery, K. O. (1973). Structural framework of Sunda shelf. *American Association of Petroleum Geologists Bulletin*, *57*(12), 2323–2366.

Ben-Avraham, Z., & Uyeda, S. (1973). The evolution of the China Basin and the Mesozoic paleogeography of Borneo. *Earth and Planetary Science Letters*, *18*(2), 365–376. https://doi.org/10.1016/0012-821X(73)90077-0

Biggin, A. J., Van Hinsbergen, D. J. J., Langereis, C. G., Straathof, G. B., & Deenen, M. H. L. (2008). Geomagnetic secular variation in the Cretaceous normal Superchron and in the Jurassic. *Physics of the Earth and Planetary Interiors*, *169*(1-4), 3–19. https://doi.org/10.1016/j.pepi.2008.07.004

Boschman, L. M., van Hinsbergen, D. J. J., Torsvik, T. H., Spakman, W., & Pindell, J. L. (2014). Kinematic reconstruction of the Caribbean region since the Early Jurassic. *Earth-Science Reviews*, *138*, 102–136. https://doi.org/10.1016/j.earscirev.2014.08.007

Boyden, J. A., Müller, R. D., Gurnis, M., Torsvik, T. H., Clark, J. A., Turner, M., et al. (2011). Next-generation plate-tectonic reconstructions using GPlates.

Breitfeld, H. T., Hall, R., Galin, T., Forster, M. A., & BouDagher-Fadel, M. K. (2017). A Triassic to Cretaceous Sundaland–Pacific subduction margin in West Sarawak, Borneo. *Tectonophysics*, *694*, 35–56. https://doi.org/10.1016/j.tecto.2016.11.034

Briais, A., Patriat, P., & Tapponnier, P. (1993). Updated interpretation of magnetic anomalies and seafloor spreading stages in the South China Sea: Implications for the Tertiary tectonics of Southeast Asia. *Journal of Geophysical Research*, *98*(B4), 6299–6328. https://doi.org/10.1029/92JB02280

Bunopas, S. (1982). Paleogeography of western Thailand and adjacent parts of Southeast Asia—A plate tectonics interpretation. *Geological Survey Division, Department of Mineral Resources Thailand*, *5*, 1–810.

Butler, R. F. (1992). *Paleomagnetism: Magnetic domains to geologic terranes*. Boston: Blackwell Scientific Publications Boston.

Chambers, J., & Daley, T. (1997). A tectonic model for the onshore Kutai Basin, East Kalimantan. In A. J. Fraser, S. J. Matthews, & R. W. Murphy (Eds.), *Petroleum geology of SE Asia*. *Geological Society of London*, 375–393.

Clements, B., Burgess, P. M., Hall, R., & Cottam, M. A. (2011). Subsidence and uplift by slab-related mantle dynamics: A driving mechanism for the Late Cretaceous and Cenozoic evolution of continental SE Asia? *Geological Society of London, Special Publication*, *355*(1), 37–51. https://doi.org/10.1144/SP355.3

Cloke, I. R., Moss, S. J., & Craig, J. (1999). Structural controls on the evolution of the Kutai Basin, East Kalimantan. *Journal of Asian Earth Sciences*, *17*(1-2), 137–156. https://doi.org/10.1016/S0743-9547(98)00036-1

Cole, J. M., & Crittenden, S. (1997). Early Tertiary basin formation and the development of lacustrine and quasi-lacustrine/marine source rocks on the Sunda shelf of SE Asia. *Geological Society of London, Special Publication*, *126*(1), 147–183. https://doi.org/10.1144/GSL.SP.1997.126.01.12

Cottam, M. A., Hall, R., & Ghani, A. A. (2013). Late Cretaceous and Cenozoic tectonics of the Malay Peninsula constrained by thermochronology. *Journal of Asian Earth Sciences*, *76*, 241–257. https://doi.org/10.1016/j.jseaes.2013.04.029

Cullen, A. B., Zechmeister, M. S., Elmore, R. D., & Pannalal, S. J. (2012). Paleomagnetism of the Crocker formation, northwest Borneo: Implications for late Cenozoic tectonics. *Geosphere*, *8*(5), 1146–1169. https://doi.org/10.1130/GES00750.1

Davies, L., Hall, R., & Armstrong, R. (2014). Cretaceous crust in SW Borneo: Petrological, geochemical and geochronological constraints from the Schwaner Mountains.
Deenen, M. H. L., Langereis, C. G., van Hinsbergen, D. J. J., & Biggin, A. J. (2011). Geomagnetic secular variation and the statistics of palaeomagnetic directions. *Geophysical Journal International*, *186*(2), 509–520. https://doi.org/10.1111/j.1365-246X.2011.05050.x
DeMets, C., Iaffaldano, G., & Merkouriev, S. (2015). High-resolution Neogene and Quaternary estimates of Nubia-Eurasia-North America plate motion. *Geophysical Journal International*, *203*(1), 416–427. https://doi.org/10.1093/gji/ggv277
Doubrovine, P. V., Steinberger, B., & Torsvik, T. H. (2012). Absolute plate motions in a reference frame defined by moving hot spots in the Pacific, Atlantic, and Indian oceans. *Journal of Geophysical Research*, *117*, B09101. https://doi.org/10.1029/2011JB009072
Fisher, R. (1953). Dispersion on a sphere, in Proceedings of the Royal Society of London A: Mathematical, Physical and Engineering Sciences. *The Royal Society*, *217*(1130), 295–305. https://doi.org/10.1098/rspa.1953.0064
François, T., Ali, M. A. M., Matenco, L., Willingshofer, E., Ng, T. F., Taib, N. I., & Shuib, M. K. (2017). Late Cretaceous extension and exhumation of the Stong and Taku magmatic and metamorphic complexes, NE Peninsular Malaysia. *Journal of Asian Earth Sciences*, *143*, 296–314. https://doi.org/10.1016/j.jseaes.2017.04.009
Fukao, Y., & Obayashi, M. (2013). Subducted slabs stagnant above, penetrating through, and trapped below the 660 km discontinuity. *Journal of Geophysical Research: Solid Earth*, *118*, 5920–5938. https://doi.org/10.1002/2013JB010466
Fukao, Y., Obayashi, M., Inoue, H., & Nenbai, M. (1992). Subducting slabs stagnant in the mantle transition zone. *Journal of Geophysical Research*, *97*(B4), 4809–4822. https://doi.org/10.1029/91JB02749
Fuller, M., Ali, J. R., Moss, S. J., Frost, G. M., Richter, B., & Mahfi, A. (1999). Paleomagnetism of Borneo. *Journal of Asian Earth Sciences*, *17*(1-2), 3–24. https://doi.org/10.1016/S0743-9547(98)00057-9
Fuller, M., Haston, R., Lin, J.-L., Richter, B., Schmidtke, E., & Almasco, J. (1991). Tertiary paleomagnetism of regions around the South China Sea. *Journal of Southeast Asian Earth Sciences*, *6*(3–4), 161–184. https://doi.org/10.1016/0743-9547(91)90065-6
Garson, M. S., & Mitchell, A. H. G. (1970). Transform faulting in the Thai peninsula. *Nature*, *228*(5266), 45–47. https://doi.org/10.1038/228045b0
Gradstein, F. M., Ogg, J. G., Schmitz, M., & Ogg, G. (2012). *The geologic time scale 2012*. Amsterdam: Elsevier.
Haile, N. S. (1973). The recognition of former subduction zones in Southeast Asia. *Implications of Continental Drift to the Earth Sciences*, *2*, 885–892.
Haile, N. S. (1974). Are the Kuantan dolerite dykes and extrusive basalt related to each other or to the Segamat basalt? Palaeomagnetic evidence. In *Geological Society of Malaysia Meeting* (pp. 25–26). Ipoh.
Haile, N. S. (1979a). Palaeomagnetic evidence for rotation and northward drift of Sumatra. *Journal of the Geological Society of London*, *136*(5), 541–546. https://doi.org/10.1144/gsjgs.136.5.0541
Haile, N. S. (1979b). Rotation of Borneo microplate completed by Miocene: Palaeomagnetic evidence. *Warta Geologi*, *5*(2), 19–22.
Haile, N. S. (1996). *Note on the Engkilili Formation and the age of the Lubok Antu Mélange*. Malaysia: West Sarawak.
Haile, N. S., Beckinsale, R. D., Chakraborty, K. R., Hussein, A. H., & Hardjono, T. (1983). Palaeomagnetism, geochronology and petrology of the dolerite dykes and basaltic lavas from Kuantan, West Malaysia: Bulletin of the Geological Society of Malaysia 16, 1983 71–85: Ill, Map.
Haile, N. S., & Khoo, H. P. (1980). Palaeomagnetic measurements on Upper Jurassic to Lower Cretaceous sedimentary rocks from Peninsular Malaysia. *Bulletin. Geological Society of Malaysia*, *12*, 75–78.
Haile, N. S., McElhinny, M. W., & McDougall, I. (1977). Palaeomagnetic data and radiometric ages from the Cretaceous of West Kalimantan (Borneo), and their significance in interpreting regional structure. *Journal of the Geological Society of London*, *133*(2), 133–144. https://doi.org/10.1144/gsjgs.133.2.0133
Hall, R. (1996). Reconstructing Cenozoic SE Asia. *Geological Society of London, Special Publication*, *106*(1), 153–184. https://doi.org/10.1144/GSL.SP.1996.106.01.11
Hall, R. (2002). Cenozoic geological and plate tectonic evolution of SE Asia and the SW Pacific: Computer-based reconstructions, model and animations. *Journal of Asian Earth Sciences*, *20*(4), 353–431. https://doi.org/10.1016/S1367-9120(01)00069-4
Hall, R. (2011). Australia–SE Asia collision: Plate tectonics and crustal flow. *Geological Society of London, Special Publication*, *355*(1), 75–109. https://doi.org/10.1144/SP355.5
Hall, R. (2012). Late Jurassic? Cenozoic reconstructions of the Indonesian region and the Indian Ocean. *Tectonophysics*, *570-571*, 1–41. https://doi.org/10.1016/j.tecto.2012.04.021
Hall, R., & Breitfeld, H. T. (2017). Nature and demise of the proto-South China Sea. *Bulletin. Geological Society of Malaysia*, *63*, 61–76.
Hall, R., Clements, B., & Smyth, H. R. (2009). Sundaland: Basement character, structure and plate tectonic development
Hall, R., Cloke, I. R., Nur'aini, S., Puspita, S. D., Calvert, S. J., & Elders, C. F. (2009). The North Makassar Straits: What lies beneath? *Petroleum Geoscience*, *15*(2), 147–158. https://doi.org/10.1144/1354-079309-829
Hall, R., & Morley, C. K. (2004). Sundaland basins. *Continent-Ocean Interactions Within East Asian Marginal Seas*, 55–85. https://doi.org/10.1029/149GM04
Hall, R., & Nichols, G. (2002). Cenozoic sedimentation and tectonics in Borneo: Climatic influences on orogenesis. *Geological Society of London, Special Publication*, *191*(1), 5–22. https://doi.org/10.1144/GSL.SP.2002.191.01.02
Hall, R., & Spakman, W. (2015). Mantle structure and tectonic history of SE Asia. *Tectonophysics*, *658*, 14–45. https://doi.org/10.1016/j.tecto.2015.07.003
Hall, R., van Hattum, M. W. A., & Spakman, W. (2008). Impact of India–Asia collision on SE Asia: The record in Borneo. *Tectonophysics*, *451*(1-4), 366–389. https://doi.org/10.1016/j.tecto.2007.11.058
Hamilton, W. B. (1979). Tectonics of the Indonesian region, US Govt. Print. Off.
Harbury, N. A., Jones, M. E., Audley-Charles, M. G., Metcalfe, I., & Mohamed, K. R. (1990). Structural evolution of Mesozoic Peninsular Malaysia. *Journal of the Geological Society of London*, *147*(1), 11–26. https://doi.org/10.1144/gsjgs.147.1.0011
Harun, Z. (2002). Late Mesozoic-early Tertiary faults of Peninsular Malaysia. *Bulletin of the Geological Society of Malaysia*, *45*, 117–120.
Hennig, J., Breitfeld, H. T., Hall, R., & Nugraha, A. M. S. (2017). The Mesozoic tectono-magmatic evolution at the paleo-Pacific subduction zone in West Borneo. *Gondwana Research*, *48*, 292–310. https://doi.org/10.1016/j.gr.2017.05.001
Heryanto, R., Supriatna, S., Rustandi, E., & Baharuddin (1994). Geological map of the Sampanahan Quadrangle, Kalimantan, 1:250,000, Geological Research and Development Centre.
Hutchison, C. S. (1989). *Geological evolution of South-east Asia*. Oxford: Clarendon Press Oxford.
Hutchison, C. S. (1996). The 'Rajang accretionary prism' and 'Lupar Line' problem of Borneo. *Geological Society of London, Special Publication*, *106*(1), 247–261. https://doi.org/10.1144/GSL.SP.1996.106.01.16
Hutchison, C. S. (1986). Formation of marginal seas by rifting of the Chinese and Australian continental margins and implications for the Borneo region. *The Bulletin of the Geological Society of Malaysia*, *20*, 201–220.

Jasin, B. (1992). Significance of radiolarian chert from the chert-Spilite formation, Telupid, Sabah [J]. *Bulletin. Geological Society of Malaysia*, *31*, 67–84.

Jasin, B., & Haile, N. S. (1993). Some radiolaria from the chert block of Lubok Antu Mélange, Sarawak.

Johnson, C. L., Constable, C. G., Tauxe, L., Barendregt, R., Brown, L. L., Coe, R. S., et al. (2008). Recent investigations of the 0–5 Ma geomagnetic field recorded by lava flows. *Geochemistry, Geophysics, Geosystems*, *9*, Q04032. https://doi.org/10.1029/2007GC001696

Kanjanapayont, P., Grasemann, B., Edwards, M. A., & Fritz, H. (2012). Quantitative kinematic analysis within the Khlong Marui shear zone, southern Thailand. *Journal of Structural Geology*, *35*, 17–27. https://doi.org/10.1016/j.jsg.2011.12.002

Kanjanapayont, P., Klötzli, U., Thöni, M., Grasemann, B., & Edwards, M. A. (2012). Rb–Sr, Sm–Nd, and U–Pb geochronology of the rocks within the Khlong Marui shear zone, southern Thailand. *Journal of Asian Earth Sciences*, *56*, 263–275. https://doi.org/10.1016/j.jseaes.2012.05.029

Kirschvink, J. L. (1980). The least-squares line and plane and the analysis of palaeomagnetic data. *Geophysical Journal International*, *62*(3), 699–718. https://doi.org/10.1111/j.1365-246X.1980.tb02601.x

Koulakov, I. (2013). Studying deep sources of volcanism using multiscale seismic tomography. *Journal of Volcanology and Geothermal Research*, *257*, 205–226. https://doi.org/10.1016/j.jvolgeores.2013.03.012

Koymans, M. R., Langereis, C. G., Pastor-Galán, D., & van Hinsbergen, D. J. J. (2016). Paleomagnetism.org: An online multi-platform open source environment for paleomagnetic data analysis. *Computational Geosciences*, *93*, 127–137. https://doi.org/10.1016/j.cageo.2016.05.007

Krähenbuhl, R. (1991). Magmatism, tin mineralization and tectonics of the Main Range, Malaysian peninsula: Consequences for the plate tectonic model of Southeast Asia based on Rb–Sr, K–Ar and fission track data. *Bulletin. Geological Society of Malaysia*, *29*, 1–100.

Lacassin, R., Leloup, P. H., & Tapponnier, P. (1993). Bounds on strain in large Tertiary shear zones of SE Asia from boudinage restoration. *Journal of Structural Geology*, *15*(6), 677–692. https://doi.org/10.1016/0191-8141(93)90055-F

Lee, T.-Y., & Lawver, L. A. (1995). Cenozoic plate reconstruction of Southeast Asia. *Tectonophysics*, *251*(1-4), 85–138. https://doi.org/10.1016/0040-1951(95)00023-2

Lefevre, J. C., Collart, M., Joubert, M., Nagel, J. L., & Paupy, A. (1982). Geological mapping and mineral exploration in north-east Kalimantan. *Rapp. BRGM*, *82*.

Leong, K. M. (1977). New ages from radiolarian cherts of the Chert-Spilite formation, Sabah. *Bulletin of the Geological Society of Malaysia*, *8*, 109–111.

Li, S., Advokaat, E. L., van Hinsbergen, D. J. J., Koymans, M., Deng, C., & Zhu, R. (2017). Paleomagnetic constraints on the Mesozoic-Cenozoic paleolatitudinal and rotational history of Indochina and South China: Review and updated kinematic reconstruction. *Earth-Science Reviews*, *171*, 58–77. https://doi.org/10.1016/j.earscirev.2017.05.007

Liew, T. C., & McCulloch, M. T. (1985). Genesis of granitoid batholiths of Peninsular Malaysia and implications for models of crustal evolution: Evidence from a Nd-Sr isotopic and U-Pb zircon study. *Geochimica et Cosmochimica Acta*, *49*(2), 587–600. https://doi.org/10.1016/0016-7037(85)90050-X

Liew, T. C., & Page, R. W. (1985). U-Pb zircon dating of granitoid plutons from the West Coast Province of Peninsular Malaysia. *Journal of the Geological Society of London*, *142*(3), 515–526. https://doi.org/10.1144/gsjgs.142.3.0515

Lippert, P. C., Van Hinsbergen, D. J. J., & Dupont-Nivet, G. (2014). Early Cretaceous to present latitude of the central proto-Tibetan Plateau: A paleomagnetic synthesis with implications for Cenozoic tectonics, paleogeography, and climate of Asia. *Geological Society of America Special Papers*, *507*, 1–21.

Lumadyo, E., McCabe, R., Harder, S., & Lee, T. (1993). Borneo: A stable portion of the Eurasian margin since the Eocene. *Journal of Southeast Asian Earth Sciences*, *8*(1–4), 225–231. https://doi.org/10.1016/0743-9547(93)90024-J

Marshall, N., Novak, V., Cibaj, I., Krijgsman, W., Renema, W., Young, J., et al. (2015). Dating Borneo's deltaic deluge: Middle Miocene progradation of the Mahakam Delta. *PALAIOS*, *30*(1), 7–25. https://doi.org/10.2110/palo.2013.066

McClay, K., Dooley, T., Ferguson, A., & Poblet, J. (2000). Tectonic evolution of the Sanga Sanga block, Mahakam Delta, Kalimantan, Indonesia. *American Association of Petroleum Geologists Bulletin*, *84*(6), 765–786.

McElhinny, M. W. (1974). Palaeomagnetic evidence shows Malay Peninsula was not a part of Gondwanaland. *Nature*, *252*(5485), 641–645. https://doi.org/10.1038/252641a0

McFadden, P. L. (1990). A new fold test for palaeomagnetic studies. *Geophysical Journal International*, *103*(1), 163–169. https://doi.org/10.1111/j.1365-246X.1990.tb01761.x

Metcalfe, I. (1990). Allochthonous terrane processes in Southeast Asia [and discussion]. *Philosophical Transactions of the Royal Society A - Mathematical Physical and Engineering Sciences*, *331*(1620), 625–640. https://doi.org/10.1098/rsta.1990.0094

Metcalfe, I. (2013). Gondwana dispersion and Asian accretion: Tectonic and palaeogeographic evolution of eastern Tethys. *Journal of Asian Earth Sciences*, *66*, 1–33. https://doi.org/10.1016/j.jseaes.2012.12.020

Monnier, C., Polvé, M., Girardeau, J., Pubellier, M., Maury, R., Bellon, H., & Permana, H. (1999). Extensional to compressive Mesozoic magmatism at the SE Eurasia margin as recorded from the Meratus ophiolite (SE Borneo, Indonesia). *Geodinamica Acta*, *12*(1), 43–55. https://doi.org/10.1080/09853111.1999.11105330

Morgan, B. A. (1974). Chemistry and mineralogy of garnet pyroxenites from Sabah, Malaysia. *Contributions to Mineralogy and Petrology*, *48*(4), 301–314. https://doi.org/10.1007/BF00951337

Morley, C. K. (2002). A tectonic model for the Tertiary evolution of strike–slip faults and rift basins in SE Asia. *Tectonophysics*, *347*(4), 189–215. https://doi.org/10.1016/S0040-1951(02)00061-6

Moss, S. J. (1998). Embaluh group turbidites in Kalimantan: Evolution of a remnant oceanic basin in Borneo during the Late Cretaceous to Palaeogene. *Journal of the Geological Society of London*, *155*(3), 509–524. https://doi.org/10.1144/gsjgs.155.3.0509

Moss, S. J., Chambers, J., Cloke, I., Satria, D., Ali, J. R., Baker, S., et al. (1997). New observations on the sedimentary and tectonic evolution of the Tertiary Kutai Basin, East Kalimantan. *Geological Society of London, Special Publication*, *126*(1), 395–416. https://doi.org/10.1144/GSL.SP.1997.126.01.24

Mullender, T. A. T., Frederichs, T., Hilgenfeldt, C., de Groot, L. V., Fabian, K., & Dekkers, M. J. (2016). Automated paleomagnetic and rock magnetic data acquisition with an in-line horizontal "2G" system. *Geochemistry, Geophysics, Geosystems*, *17*, 3546–3559. https://doi.org/10.1002/2016GC006436

Otofuji, Y., Moriyama, Y. T., Arita, M. P., Miyazaki, M., Tsumura, K., Yoshimura, Y., et al. (2017). Tectonic evolution of the Malay Peninsula inferred from Jurassic to Cretaceous paleomagnetic results. *Journal of Asian Earth Sciences*, *134*, 130–149. https://doi.org/10.1016/j.jseaes.2016.10.007

Parkinson, C. D., Miyazaki, K., Wakita, K., Barber, A. J., & Carswell, D. A. (1998). An overview and tectonic synthesis of the pre-Tertiary very-high-pressure metamorphic and associated rocks of Java, Sulawesi and Kalimantan, Indonesia. *Island Arc*, *7*(1–2), 184–200. https://doi.org/10.1046/j.1440-1738.1998.00184.x

Pesicek, J. D., Thurber, C. H., Zhang, H., DeShon, H. R., Engdahl, E. R., & Widiyantoro, S. (2010). Teleseismic double-difference relocation of earthquakes along the Sumatra-Andaman subduction zone using a 3-D model. *Journal of Geophysical Research*, *115*, B10303. https://doi.org/10.1029/2010JB007443

Priyomarsono, S. (1985). *Contribution a l'etude geologique du Sud-est de Borneo, Indonesia: Geologie structurale de la partie meridionale de la chaine des Meratus*. Chambery: Université de Savoie.

Pueyo, E. L., Parés, J. M., Millán, H., & Pocovı, A. (2003). Conical folds and apparent rotations in paleomagnetism (a case study in the southern Pyrenees). *Tectonophysics*, *362*(1-4), 345–366. https://doi.org/10.1016/S0040-1951(02)00645-5

Rangin, C., Bellon, H., Benard, F., Letouzey, J., Muller, C., & Sanudin, T. (1990). Neogene arc-continent collision in Sabah, northern Borneo (Malaysia). *Tectonophysics*, *183*(1–4), 305–319. https://doi.org/10.1016/0040-1951(90)90423-6

Renema, W., Warter, V., Novak, V., Young, J. R., Marshall, N., & Hasibuan, F. (2015). Ages of Miocene fossil localities in the northern Kutai Basin (East Kalimantan, Indonesia). *PALAIOS*, *30*(1), 26–39. https://doi.org/10.2110/palo.2013.127

Replumaz, A., Kárason, H., van der Hilst, R. D., Besse, J., & Tapponnier, P. (2004). 4-D evolution of SE Asia's mantle from geological reconstructions and seismic tomography. *Earth and Planetary Science Letters*, *221*(1-4), 103–115. https://doi.org/10.1016/S0012-821X(04)00070-6

Replumaz, A., & Tapponnier, P. (2003). Reconstruction of the deformed collision zone between India and Asia by backward motion of lithospheric blocks. *Journal of Geophysical Research*, *108*(B6), 2285. https://doi.org/10.1029/2001JB000661

Richter, B., Schmidtke, E., Fuller, M., Harbury, N., & Samsudin, A. R. (1999). Paleomagnetism of Peninsular Malaysia. *Journal of Asian Earth Sciences*, *17*(4), 477–519. https://doi.org/10.1016/S1367-9120(99)00006-1

Ridd, M. F., & Watkinson, I. (2013). The Phuket-Slate Belt terrane: Tectonic evolution and strike-slip emplacement of a major terrane on the Sundaland margin of Thailand and Myanmar. *Proceedings of the Geologists Association*, *124*(6), 994–1010. https://doi.org/10.1016/j.pgeola.2013.01.007

Royden, L. H., Burchfiel, B. C., & van der Hilst, R. D. (2008). The geological evolution of the Tibetan Plateau. *Science*, *321*(5892), 1054–1058. https://doi.org/10.1126/science.1155371

Rutten, M. G. (1940). On Devonian limestones with *Clathrodictyon* cf. *spatiosum* and *Heliolites porosus* from eastern Borneo. *Proceedings of the Koninklijke Nederlandse Akademie van Wetenschappen Amsterdam*, *43*, 1061–1064.

Sasajima, S., Otofuji, Y., Hirooka, K., Suparka, S., & Hehuwat, F. (1978). Palaeomagnetic studies on Sumatra Island and the possibility of Sumatra being part of Gondwanaland. *Rockmagnetism and Paleogeophys*, *5*, 104–110.

Schmidtke, E., Dunn, J. R., Fuller, M., & Haston, R. (1985). Preliminary paleomagnetic results from Sabah: East Malaysia. *Eos, Transactions American Geophysical Union*, *66*, 864.

Schmidtke, E. A., Fuller, M. D., & Haston, R. B. (1990). Paleomagnetic data from Sarawak, Malaysian Borneo, and the late Mesozoic and Cenozoic tectonics of Sundaland. *Tectonics*, *9*(1), 123–140. https://doi.org/10.1029/TC009i001p00123

Setiawan, N. I., Osanai, Y., Nakano, N., Adachi, T., Setiadji, L. D., & Wahyudiono, J. (2013). Late Triassic metatonalite from the Schwaner Mountains in West Kalimantan and its contribution to sedimentary provenance in the Sundaland. *Berita Sedimentologi*, *12*, 4–12.

Seton, M., Müller, R. D., Zahirovic, S., Gaina, C., Torsvik, T., Shephard, G., et al. (2012). Global continental and ocean basin reconstructions since 200 Ma. *Earth-Science Reviews*, *113*(3-4), 212–270. https://doi.org/10.1016/j.earscirev.2012.03.002

Shao, L., Cao, L., Ojao, P., Zhang, X., Li, Q., & van Hinsbergen, D. J. J. (2017). Cretaceous–Eocene provenance connections between the Palawan continental terrane and the northern South China Sea margin. *Earth and Planetary Science Letters*, *477*, 97–107. https://doi.org/10.1016/j.epsl.2017.08.019

Sikumbang, N. (1986). *Geology and tectonics of pre-Tertiary rocks in the Meratus Mountains south-east Kalimantan*. Indonesia: University of London.

Sikumbang, N., & Heryanto, R. (1994). Peta Geologi Lembar Banjarmasin, Kalimantan Selatan skala 1: 250.000, *Pus. Penelit. dan Pengemb. Geol. Bandung*.

Smyth, H. R., Hall, R., & Nichols, G. J. (2008). Cenozoic volcanic arc history of East Java, Indonesia: the stratigraphic record of eruptions on an active continental margin. *Special Papers-Geological Society of America*, *436*, 199–222

Soeria-Atmadja, R., Maury, R. C., Bellon, H., Pringgoprawiro, H., Polve, M., & Priadi, B. (1994). Tertiary magmatic belts in Java. *Journal of Southeast Asian Earth Sciences*, *9*(1–2), 13–27. https://doi.org/10.1016/0743-9547(94)90062-0

Sugiaman, F., & Andria, L. (1999). Devonian carbonate of Telen River, East Kalimantan. *Ber. Sedimentol.*, *10*, 18–19.

Sunata, W., & Permanadewi, S. (1998). Data magnet purba dan penarikhan Kalium-Argon dari batuan mikrodiorit Gunung Kukusan utara, daerah Batulicin, Kalimantan Selatan. *Pusat Penelitian dan Pengembangan Geologi, Bandung* (pp. 260–268). Bandung.

Sunata, W., & Wahyono, H. (1987). APWP untuk Kalimantan Barat, in Abstract at the annual Geological Research and Development Centre Colloquium (Paleomagnetics of igneous rocks of Putussibau, West Kalimantan).

Sunata, W., & Wahyono, H. (1998). Data magnet purba teruji untuk formasi Tanjung, daerah Batulicin, Kalimantan Selatan; dan aplikasinya untuk menentukan waktu Terjadinya rotasi. *Pusat Penelitian dan Pengembangan Geologi*.

Sunata, W., Wahyono, H., & Sanyoto, P. (1987). Magnet Purbadari beberapa batuan beku di daerah Putussibau, Kalimantan Barat. Abstract at the Annual Geological Research and Development Centre colloquium, Bandung.

Tan, D. N. K. (1979). Lupar Valley, West Sarawak; explanation of sheets 1-111-14, 1-111-15, and 1-111-16. *Geological Survey of Malaysia Report*, *13*, 1–159.

Tan, D. N. K. (1982). The Lubok Antu Melange, Lupar Valley West Sarawak a lower Tertiary subduction complex. *Bulletin. Geological Society of Malaysia*, *15*, 31–46.

Tapponnier, P., Peltzer, G., & Armijo, R. (1986). On the mechanics of the collision between India and Asia. *Geological Society of London, Special Publication*, *19*(1), 113–157. https://doi.org/10.1144/GSL.SP.1986.019.01.07

Tjia, H. D. (1996). Tectonics of deformed and undeformed Jurassic-Cretaceous strata of Peninsular Malaysia. *Bulletin. Geological Society of Malaysia*, *39*, 131–156.

Tongkul, F. (1994). The geology of northern Sabah, Malaysia: Its relationship to the opening of the South China Sea basin. *Tectonophysics*, *235*(1–2), 131–147. https://doi.org/10.1016/0040-1951(94)90021-3

Tongkul, F. (2006). The structural style of Lower Miocene sedimentary rocks, Kudat Peninsula, Sabah. *Bulletin of the Geological Society of Malaysia*, *49*, 119–124.

Torsvik, T. H., Van der Voo, R., Preeden, U., Mac Niocaill, C., Steinberger, B., Doubrovine, P. V., et al. (2012). Phanerozoic polar wander, palaeogeography and dynamics. *Earth-Science Reviews*, *114*(3-4), 325–368. https://doi.org/10.1016/j.earscirev.2012.06.007

van de Weerd, A. A., & Armin, R. A. (1992). Origin and evolution of the Tertiary hydrocarbon-bearing basins in Kalimantan (Borneo), Indonesia (1). *American Association of Petroleum Geologists Bulletin*, *76*(11), 1778–1803.

van der Meer, D., van Hinsbergen, D. J. J., & Spakman, W. (2017). Atlas of the underworld: Slab remnants in the mantle, their sinking history, and a new outlook on lower mantle viscosity. *Tectonophysics*, *723*, 309–448. https://doi.org/10.1016/j.tecto.2017.10.004

Van der Voo, R. (1990). The reliability of paleomagnetic data. *Tectonophysics*, *184*(1), 1–9.
Van Hattum, M. W. A., Hall, R., Pickard, A. L., & Nichols, G. J. (2013). Provenance and geochronology of Cenozoic sandstones of northern Borneo. *Journal of Asian Earth Sciences*, *76*, 266–282. https://doi.org/10.1016/j.jseaes.2013.02.033
Van Hinsbergen, D. J. J., Kapp, P., Dupont-Nivet, G., Lippert, P. C., DeCelles, P. G., & Torsvik, T. H. (2011). Restoration of Cenozoic deformation in Asia and the size of greater India. *Tectonics*, *30*, TC5003. https://doi.org/10.1029/2011TC002908
van Hinsbergen, D. J. J., Lippert, P. C., Li, S., Huang, W., Advokaat, E. L., & Spakman, W. (2018). Reconstructing greater India: Paleogeographic, kinematic, and geodynamic perspectives. *Tectonophysics*. https://doi.org/10.1016/j.tecto.2018.04.006
Wahyono, H., & Sunata, W. (1987). Palaeomagnetism along transect VII, Jt. CCOP/IOC Work. Gr. SEATAR 1987 Prelim. Rep. Jawa-Kalimantan Transect (Transect VII), 1–10.
Wakita, K., Miyazaki, K., Zulkarnain, I., Sopaheluwakan, J., & Sanyoto, P. (1998). Tectonic implications of new age data for the Meratus Complex of South Kalimantan, Indonesia. *Island Arc*, *7*(1–2), 202–222. https://doi.org/10.1046/j.1440-1738.1998.00163.x
Watkinson, I. (2009). The kinematic history of the Khlong Marui and Ranong faults, southern Thailand, University of London.
Watkinson, I., Elders, C., Batt, G., Jourdan, F., Hall, R., & McNaughton, N. J. (2011). The timing of strike-slip shear along the Ranong and Khlong Marui faults, Thailand. *Journal of Geophysical Research*, *116*, B09403. https://doi.org/10.1029/2011JB008379
Watkinson, I., Elders, C., & Hall, R. (2008). The kinematic history of the Khlong Marui and Ranong faults, southern Thailand. *Journal of Structural Geology*, *30*(12), 1554–1571. https://doi.org/10.1016/j.jsg.2008.09.001
Whittaker, J. M., Müller, R. D., Leitchenkov, G., Stagg, H., Sdrolias, M., Gaina, C., & Goncharov, A. (2007). Major Australian-Antarctic plate reorganization at Hawaiian-Emperor bend time. *Science*, *318*(5847), 83–86. https://doi.org/10.1126/science.1143769
Widiyantoro, S., Pesicek, J. D., & Thurber, C. H. (2011). Subducting slab structure below the eastern Sunda arc inferred from non-linear seismic tomographic imaging. *Geological Society of London, Special Publication*, *355*(1), 139–155. https://doi.org/10.1144/SP355.7
Widiyantoro, S., & van der Hilst, R. (1996). Structure and evolution of lithospheric slab beneath the Sunda arc, Indonesia. *Science*, *271*(5255), 1566–1570. https://doi.org/10.1126/science.271.5255.1566
Widiyantoro, S., & van der Hilst, R. (1997). Mantle structure beneath Indonesia inferred from high-resolution tomographic imaging. *Geophysical Journal International*, *130*(1), 167–182. https://doi.org/10.1111/j.1365-246X.1997.tb00996.x
Williams, P. R., & Harahap, B. H. (1987). Preliminary geochemical and age data from postsubduction intrusive rocks, Northwest Borneo. *Australian Journal of Earth Sciences*, *34*(4), 405–415. https://doi.org/10.1080/08120098708729422
Williams, P. R., Johnston, C. R., Almond, R. A., & Simamora, W. H. (1988). Late Cretaceous to early Tertiary structural elements of West Kalimantan. *Tectonophysics*, *148*(3–4), 279–297. https://doi.org/10.1016/0040-1951(88)90135-7
Williams, P. R., Supriatna, S., & Harahap, B. (1986). Cretaceous melange in West Kalimantan and its tectonic implications. *Bulletin. Geological Society of Malaysia*, *19*, 69–78.
Witts, D., Hall, R., Morley, R. J., & BouDagher-Fadel, M. K. (2011). Stratigraphy and sediment provenance, Barito basin, Southeast Kalimantan
Witts, D., Hall, R., Nichols, G., & Morley, R. (2012). A new depositional and provenance model for the Tanjung formation, Barito Basin, SE Kalimantan, Indonesia. *Journal of Asian Earth Sciences*, *56*, 77–104. https://doi.org/10.1016/j.jseaes.2012.04.022
Wu, J., & Suppe, J. (2017). Proto-South China Sea plate tectonics using subducted slab constraints from tomography. *Journal of Earth Science*, 1–15.
Yuwono, Y. S., Priyomarsono, S., Maury, T. R. C., Rampnoux, J. P., Soeria-Atmadja, R., Bellon, H., & Chotin, P. (1988). Petrology of the Cretaceous magmatic rocks from Meratus Range, southeast Kalimantan. *Journal of Southeast Asian Earth Sciences*, *2*(1), 15–22. https://doi.org/10.1016/0743-9547(88)90017-7
Zijderveld, J. D. A. (1967). AC demagnetization of rocks: Analysis of results. *Methods in Paleomagnetism*, *1*, 254–286.